NASA CONTRACTOR REPORT

NASA CR-1090

NASA CR-1090

GPO PRICE $ _____

CFSTI PRICE(S) $ _____

Hard copy (HC) 3.00

Microfiche (MF) .65

653 July 65

FACILITY FORM 602

N68-28373 (ACCESSION NUMBER) (THRU)

95 (PAGES) 1 (CODE)

(NASA CR OR TMX OR AD NUMBER) 30 (CATEGORY)

ULTRAHIGH VACUUM ADHESION RELATED TO THE LUNAR SURFACE

Prepared by

DOUGLAS AIRCRAFT COMPANY
Santa Monica, Calif.

for

NATIONAL AERONAUTICS AND SPACE ADMINISTRATION • WASHINGTON, D. C. • JULY 1968

NASA CR-1090

ULTRAHIGH VACUUM ADHESION RELATED TO THE LUNAR SURFACE

Prepared under Contract No. NAS 7-307 by
DOUGLAS AIRCRAFT COMPANY
Santa Monica, Calif.

for

NATIONAL AERONAUTICS AND SPACE ADMINISTRATION

For sale by the Clearinghouse for Federal Scientific and Technical Information
Springfield, Virginia 22151 – CFSTI price $3.00

TABLE OF CONTENTS

Abstract		v
1.0	INTRODUCTION AND SUMMARY	1
	1.1 General	1
	1.2 Purpose and Importance of Program	1
	1.3 Approach	1
	1.4 Work Accomplished During First Year	2
	1.5 Work Accomplished During Second Year	3
	1.6 Work Accomplished During Third Year	4
	1.7 Items of Note	4
2.0	THE SILICATES	5
3.0	NATURE OF SILICATE SURFACES	8
4.0	POSSIBLE ADHESION PRODUCING FORCES	9
5.0	LUNAR SURFACE ADHESION	12
6.0	PREVIOUS RELATED WORK	14
7.0	SAMPLE CHOICE AND PREPARATION	16
	7.1 Sample Choice	16
	7.2 Sample Preparation	17
	7.2.1 Silicates and Non-Metallic Non-Silicates	17
	7.2.2 Air-Formed Metals	20
8.0	INSTRUMENTATION	20
	8.1 Vacuum System	20
	8.2 Load Application System	21
	8.3 Adhesion Measuring System	22
	8.3.1 Adhesion of Air-Formed Surfaces	22
	8.3.2 Adhesion of Vacuum-Formed Surfaces	22
	8.4 Cleavage Devices	23

9.0 EXPERIMENTAL DATA 23

9.1 Adhesion Between Air-Formed Surfaces 23

9.1.1 Silicate-Silicate 23
9.1.2 Silicate-Non-Silicate 33

9.2 Adhesion Between Vacuum Cleaved Surfaces 33

9.2.1 Single Cleavage 33
9.2.2 Double Cleavage 54

10.1 DISCUSSION OF DATA 62

10.1 Air-Formed Surfaces 62

10.1.1 Silicate-Silicate Contact 62
10.1.2 Silicate-Non-Silicate Contact 69

10.2 Vacuum-Cleaved Surfaces 71

10.2.1 Single Cleavage 71
10.2.2 Double Cleavage 75
10.2.3 Origin and Nature of Long Range Force 76

10.2.3.1 Crystal Imperfections 77
10.2.3.2 Non-Uniform Composition 78
10.2.3.3 Work Function 79

10.2.4 Source of Gas Bursts 79

11.0 IMPLICATIONS OF RESULTS TO THE MOON 81

11.1 Lunar Soil Mechanics 81
11.2 General Problems to Engineering Operations 83

12.0 CONCLUSIONS 86

REFERENCES 88

ABSTRACT

This report presents a summary of results obtained during the past three years on a study of the ultrahigh vacuum adhesion of silicates as related to the lunar surface. Emphasis is given to the results obtained during the third year, particularly the last quarter which has not previously been reported.

Silicates, such as may exist at the lunar surface, were contacted with silicates and with engineering materials that may be used at the lunar surface. Adhesion variables studied were effects of type of material, degree of surface cleanliness, surface roughness, load force, crystalline orientation, and temperature.

The silicate surfaces to be contacted were in some cases formed in air, in other cases they were formed at ultrahigh vacuum by cleavage. These two types of surface formation were chosen to represent bounds to the possible range of surface states existing on the moon: the first type representing a contaminated surface, the second an ultraclean surface.

It was found that the adhesion phenomena observed were critically dependent upon the surface state. Two types of adhesion were noted for the air-formed surfaces. The first appeared only at ultrahigh vacuum, was of relatively high magnitude, was highly load dependent, and produced extensive surface damage and material transfer. The second type was of relatively low magnitude and appeared under low load and touch contact. It is concluded that the first type is caused by the action of the normal atomic bonding

forces, whereas the second type is produced through the action of dispersion forces.

The adhesion between ultrahigh vacuum-formed silicate surfaces was orders of magnitude greater than that between the air-formed surfaces. In addition, a strong long range attractive force, indicative of surface charging, was noted. This force was sufficiently strong to pull the samples into contact for separations up to 2 mm. Additionally, the force field was macroscopically anisotropic, being able to physically rotate and translate the samples into preferred positions of contact. It is concluded that the highest magnitude adhesion may be caused through the action of the normal atomic bonding forces, but the surface charging makes a significant contribution. Also, it is concluded that though random charge separation associated with bond breakage could contribute to surface charging, the major contributors are the defect structures in the crystal lattice.

Since silicate adhesion is critically dependent upon surface state, it is obviously unwise to make any general statement regarding the degree of adhesion to be expected during lunar missions. The adhesion found, and the problems it produces, will depend importantly upon the present state of the lunar material surfaces and upon how a specific operation affects this surface state.

1.0 INTRODUCTION AND SUMMARY

1.1 General

This report presents a summary of work accomplished during the period July 1, 1964 through July 1, 1967 on the study of the ultrahigh vacuum frictional-adhesional behavior of silicates as related to the lunar surface.

1.2 Purpose and Importance of Program

The primary purposes of this program are 1) to obtain quantitative experimental data concerning the ultrahigh vacuum adhesional-frictional behavior of the materials which may presently exist at the lunar surface (primarily silicates), and between these and engineering materials which may be placed upon this surface, and 2) to use these data to obtain a better understanding of the mechanisms of adhesion. Additional purposes are to analyze these data with regard to the possible reactions of granular lunar materials to engineering operations, and to investigate means by which the problems, if any, posed by these reactions may be minimized.

The importance of this program is that adhesional-frictional phenomena may pose serious problems to lunar surface operations.

1.3 Approach

The approach used during the first year of the study was to obtain quantitative data relating to the adhesion force between air-formed (contaminated) surfaces at ultrahigh vacuum as a function of type of material, load force, crystalline orientation, and temperature.

The approach used during the second year of the study was to obtain additional data in the manner of the previous year, investigate the effects of forepump type and surface roughness on the adhesion, and check data reproducibility.

The approach used during the third year of the study was to produce various silicate surfaces at ultrahigh vacuum by cleavage ("clean" surfaces), contact like and unlike surfaces and measure the adhesion force. The third year approach was chosen to investigate how the adhesion of "clean" silicate surfaces may differ from that between "dirty" silicate surfaces, and hence determining possible bounds to lunar adhesional phenomena.

1.4 Work Accomplished During First Year

Silicates, such as may exist at the lunar surface, were contacted with silicates and with engineering materials which may be used at the lunar surface. The adhesion was measured as a function of load force, temperature, and type of material. Load forces up to about 10^6 dynes were applied; temperature was varied from about 100°K to about 400°K, approximately the lunar temperature range. Adhesion as small as 2×10^{-2} dynes could be detected. Materials used were orthoclase, albite, bytownite, hornblende, hypersthene, and obsidian among the silicates; aluminum, magnesium, titanium alloy, and beryllium among the metals; alumina and a commercial glass. A definite load dependence for the adhesion was detected. For some samples no adhesion was detected at low loadings, but as load was increased the adhesion increased rapidly to relatively large values (generally hundreds of dynes). All evidence indicated that this behavior was produced by the action of the normal atomic bonding forces. For other samples, however, adhesion was present at low loading; it increased only slightly with increasing load, reaching a maximum value of only a few dynes at most. The evidence indicated that the dispersion forces were responsible for this behavior. No effect of temperature on the adhesion was detected. Indications of a correlation between the magnitude of the adhesion force and crystalline orientation were observed, the adhesion force reaching a maximum about the position of atomic match in orientation.

1.5 Work Accomplished During Second Year

The adhesion of additional silicates and engineering materials was studied as a function of load force, surface roughness, type of forepump used, and for checking data reproducibility. The data obtained generally confirmed the findings of the first year. Two types of adhesional behavior were found. The first appeared only under load, increasing rapidly with increasing load; was of relatively large magnitude (up to about 4×10^2 dynes); and was present only at ultra-high vacuum. In addition, when this type of adhesion was present, extensive surface damage and material transfer were noted. It was concluded that this type of behavior is caused by the action of the normal silicate atomic bonding forces. The second type was present at zero load, showed much less load dependence, was of relatively low magnitude, persisted in dry nitrogen (at atmospheric pressure), and did not produce surface damage or material transfer. It was concluded that this type of behavior is most probably caused by the action of the dispersion forces.

Further indications in this regard came from the surface roughness studies. It was found that the magnitude of the low load adhesion increased as surface roughness decreased. This is the type of behavior that would be expected if this low-load adhesion was caused by dispersion forces. It was also found that the high-load adhesion was unaffected by surface roughness, which would be expected, at least over the range of surface roughnesses used (300 $\mathring{A}$ to 8μ peak to peak), if the normal atomic bonding forces were responsible for the adhesion.

Additional data revealed that the adhesional phenomena were unaffected by the type of forepump used (liquid nitrogen trapped mechanical vs. sorption), and that these phenomena were quite reproducible.

1.6 Work Accomplished During Third Year

Various silicates were cleaved at ultrahigh vacuum, then touch contacted and the adhesion force measured. The silicates cleaved were orthoclase, labradorite, microcline, and andesine. The adhesion was measured for the two fresh surfaces produced by a single cleavage, for two dissimilar surfaces (each a different silicate) produced by double cleavage, and for similar surfaces (each the same silicate but from different samples) produced by double cleavage. It was found that the adhesion magnitude was much larger than for the air-formed surfaces, adhesion forces as large as 10^4 dynes under touch contact being recorded. The adhesion decreased rapidly during the first several minutes after cleavage following which only a very gradual further decrease occurred during the next several days. This behavior occurred regardless of whether similar or dissimilar mineral faces were contacted. Additionally, a strong long range attractive force, indicative of considerable surface electrostatic charging, was noted. This force field was found to be anisotropic on a macroscopic scale, and was present for unlike as well as like samples. It was concluded that this charging may be associated with the defect structures (dislocations and impurities) in the crystals.

1.7 Items of Note

Seven publications and presentations have resulted to date from the work under this program: Ryan and Sun (1965a and b), Ryan (1966a and b), Ryan and Baker (1967),

Ryan and Hansen (1967), and Grossman (1967). Two additional papers, to be submitted to the Journal of Geophysical Research, are in progress.

2.0 THE SILICATES

It is of interest, since the majority of effort during this study is concentrated upon the silicates, to outline briefly the physical nature of silicate systems such as occur in terrestrial and meteoritic materials.

The silicates are as a whole highly stable structures. The basic building unit of all silicates is the silica tetrahedron consisting of a silicon atom (at the center) surrounded by four oxygens (at the vertices). The silicon-oxygen bond is intermediate between a pure covalent and pure ionic type. The wide diversity within the silicate family can be explained by the varying degrees to which these oxygen atoms are shared by a second silicon, also by the fact that there are a number of other atoms which can either substitute for the silicon (such as aluminum) or can enter into the general lattice (such as potassium, sodium, calcium, barium, aluminum, and OH^- radical). On the basis of oxygen sharing the silicates are generally grouped into six classes: independent tetrahedral groups (the orthosilicates); double tetrahedral structures (dimers); ring structures; chain structures; sheet structures; and three dimensional networks. A wide variety of mineral types are found within each class due to the introduction into the lattice of various different atoms.

The general characteristics of each class are as follows:

(1) Independent Tetrahedral Groups

No oxygens are shared and each silica tetrahedron is in this sense independent of all others. The crystal integrity is maintained by bonding between the oxygens and cations other than silicon. Examples of this type of structure are olivine (an important constituent of meteorites) and the epidote group of minerals.

(2) Double Tetrahedral Structures

The tetrahedra occur in pairs with a single oxygen per pair being shared. Each pair is separated from all other pairs, the remaining oxygens bonding with cations other than silicon. An example of this type of structure is shown by hemimorphite.

(3) Ring Structures

Two oxygen atoms per tetrahedron are shared. The tetrahedra form rings containing two, three, four or six tetrahedra per ring. The remaining oxygens bond with cations other than silicon. An example of this class is beryl (six tetrahedra per ring).

(4) Chain Structures

(a) Single Chain

Two oxygens per tetrahedron are shared and the tetrahedra are joined into chairs of "infinite" extent. The chains normal to their length are bonded by means of linkages between the remaining oxygens and cations other than silicon. An example of this type of structure is given by the pyroxene group of

minerals, relatively important constituents of terrestrial igneous rocks, particularly the more basic varieties, and meteorites.

(b) Double Chains

The tetrahedra share alternately two and three oxygens forming double linked chains of "infinite" extent. The chains, normal to their length, are bonded by means of linkages between the remaining oxygens and cations other than silicon. An example of this type of structure is given by the amphibole group of minerals.

(5) Sheet Structures

Three oxygen atoms are shared per tetrahedron, the remaining oxygen bonding with cations other than silicon. The silicon bonded oxygens form parallel planes of "infinite" extent. An outstanding example of this type of structure is given by the micas, relatively common constituents of terrestrial igneous rock.

(6) Three-Dimensional Networks

All oxygens of each tetrahedra are shared with adjacent tetradehra. The diversity of minerals in this class results from the replacement of some of the silicon atoms and the introduction of additional atoms into the structure to maintain charge neutrality. An example of this type of structure is given by the feldspars, most important rock and meteorite constituents.

3.0 NATURE OF SILICATE SURFACES

The physico-chemical nature of silicate surfaces has been considered by a number of investigators. Most of this work has been summarized by Eitel [1964]. Studies of particular interest are those by Weyl [1955] and DeVore [1963]. Weyl has approached the problem from the classical electrostatic and polarization viewpoint, rather than from the quantum mechanical homopolar-bond-resonance viewpoint. Though the validity, or desirability, of approaching the problem from an essentially classical basis can be questioned, Weyl's treatment has been successful in providing reasonable explanations for a number of phenomena associated with silicate surfaces, and hence it appears that his approach is, at present, as good as any for use as a starting point in the understanding of silicate adhesion.

A freshly produced silicate surface must adjust to the resulting changed conditions, these changed conditions being the unsatisfied charge and coordinations produced and exposure to the external environment. According to Weyl there are, in general, three possible ways in which a solid surface can adjust: through polarization of surface ions, through distortion of surface structure with formation of an electric double layer, and through adsorption of materials from the surrounding environment. For silicates, the first possibility can be disregarded because of the low polarizability of the Si^{4+} (also Al^{3+}) ions. Obviously, if the new surfaces are formed in a perfect vacuum, distortion alone is possible. Surface distortion, according to Weyl, is caused by the necessity for cation screening. Hence the anions (O^{2-}) tend to displace toward the surface and the cations displace away from it. This forms oriented dipoles (electric double layer), the negative poles

being at the surface, and reduces the role of the cations in surface phenomena.

DeVore [1963] has considered further the changes occurring at a freshly produced silicate surface. He notes that in almost all cases Si-O bonds, as well as metal-oxygen bonds, must be broken. If surface formation occurs in air, the exposed silicon (or metal) ions will satisfy their charge and coordination demands by attaching oxygen, and the exposed oxygen (initial and attached) will satisfy their demands through the addition of water (as H+ to form hydroxyl groups and as adsorbed polar molecules). Essentially all silicate surfaces formed in air can therefore be considered to be hydrated. For a surface formed in vacuum, the charge and coordination demands remain unsatisfied, and, even though surface distortion occurs in an attempt to improve cation screening, the surface will remain highly reactive.

4.0 POSSIBLE ADHESION PRODUCING FORCES

There are a number of processes (or forces) that may contribute to solid-solid silicate adhesion in vacuum. These are the action of the normal silicate lattice bonding forces (ionic-covalent), the action of dispersion forces (London-Van der Waals), surface electrostatic charging, and the action of adsorbed surface films (including hydrogen bonding).

The silicate bonding forces are highly directional, and their range of effectiveness is the shortest of all forces which could act. Hence their effectiveness should be highly sensitive to the atomic structures of the contacting surfaces, to the degree of surface contamination present, and to the degree to which charge and coordination demands are unsatisfied. These forces are, in general, the only ones of sufficient strength to produce surface disruption.

The dispersion (London-Van der Waals) forces can also contribute significantly to silicate adhesion, as evidenced by the work of Bradley [1932], Lowe and Lucas [1953], Jordan [1954], and Derjaguin et al. [1954]. These forces have a range of effectiveness much greater than that of the ionic-covalent forces, but less than that of the forces produced by electrostatic surface charging. Also, unlike the ionic-covalent bonds, these forces are essentially nondirectional. The force-distance relationships for these dispersion forces have been calculated theoretically and verified experimentally for surface separations greater than about a tenth of a micron. Harper [1955] has shown that contact of quartz surfaces can produce a surface electrostatic charge In general, this charge produces long-range forces - the longest range of effectiveness of any which may act. This phenomenon is herein called 'homogeneous' surface charging as did Overbeek and Sparnaay [1954]. Another type of surface charging, called 'mosaic charging,' has been postulated by Derjaguin et al. to explain the anomalously high attractive forces detected by Overbeek and Sparnaay. According to Derjaguin et al., because no surface is perfect with respect to atomic arrangement, lack of localized impurities, etc., a mosaic distribution of charges (of opposite signs) could be generated, the net surface charge remaining zero or near zero. If a certain amount of surface mobility of these charges is allowed, forces could act between two dielectrics brought into close proximity or contact. Because of the mosaic distribution of these charges, the range of effectiveness of the forces produced would be much less than that of those produced by homogeneous surface charging but greater than the range of effectiveness of the ionic-covalent and dispersion forces.

The action of adsorbed surface films, particularly H_2O (OH), in producing solid-solid adhesion has been known for some time, a considerable amount of work having been done on this problem in the field of clay mineralogy. Grim [1953] notes that chemisorbed hydrogen (OH) bonding between the silicate units is a major contributor to the strength of clays and that adsorbed water also can contribute. As far as vacuum adhesion is concerned, however, the adsorbed water can be removed by heating to 100-150°C and possibly also by exposure to the vacuum alone. However, the chemisorbed hydrogen (OH) requires bakeout at least to 400°C, and possibly to 700°C. Hence, for surfaces produced in air, this remains a possible adhesion-producing mechanism in vacuum.

Hydrogen bonding, which in certain aspects is similar to that found in clays, is also postulated to cause adhesion through surface charging. According to Weyl's views [see Gruver, 1956], transfer of hydrogen ions (such as will become attached to silicate surfaces formed in air) can occur between contacting surfaces if the degree of cation screening of the two surfaces is dissimilar, the hydrogen ions moving from the surface having the more poorly screened cations. This will result in the formation of an electric potential between the surfaces and hence will cause adhesion. This is a possible adhesion-producing mechanism in vacuum, provided that surface-cleaning techniques are insufficient to remove hydrated surface layers, but this charging mechanism should not act for similar materials in contact.

Since a number of mechanisms could act to produce adhesion between contacting silicate surfaces in vacuum, the problem of understanding the nature of the adhesion becomes somewhat complicated. Additional complications arise from

present uncertainties regarding the nature of silicate surfaces, the specification of what a 'clean' silicate surface is and when it is 'clean,' and the determination of the proper method for removal of surface contamination.

5.0 LUNAR SURFACE ADHESION

The Surveyors have shown that adhesion occurs at the lunar surface, and that this contributes significantly to the soil strength. The Surveyors do not, however, reveal the nature of the force(s) producing this adhesion, and hence whether for all engineering operations performed the adhesion can be expected to behave similarly. The reason for this is that we do not as yet know the exact nature of the surfaces of lunar materials (it is important to know this since, as will be seen, the adhesion is critically dependent upon surface state and hence upon how engineering operations alter the surface state).

However, reasonable bounds can be placed upon surface state as pertains to the resultant adhesional behavior. The lower bound would be for surfaces whose charge and coordination demands are satisfied, and which have some degree of adsorbed material present. The upper bound would be for surfaces whose charge and coordination demands are unsatisfied (actually, this is probably a minimum upper bound since time in contact effects, on the lunar scale, are not considered).

If, during the formation of a fresh surface on the moon, an atmosphere were present, either as part of a general lunar atmosphere or as a transient phenomenon generated by the mechanism causing fresh surface production, then the charge and coordination demands could be satisfied, and some degree of

surface contamination could persist. Additionally, even if a significant atmosphere is not present at generation, it is conceivable that the surface demands could be satisfied over a period of time, either by the remnant lunar atmosphere, or by de-gassing from the lunar interior (some partial satisfaction could be produced from the hydrogen of the solar wind, but appreciable quantities of oxygen are also required for complete satisfaction). Such surfaces could exist below the lunar surface, but, if the solar wind strikes the lunar surface, it is unlikely that they could exist at the surface.

On the other hand, if a fresh surface is produced in the absence of an atmosphere, the charge and coordination demands can remain unsatisfied. Alternatively, a contaminated surface exposed to the solar wind can be "cleaned" to the extent that its demands are no longer satisfied. Such surfaces can exist at, and below, the lunar surface, being produced through the action of the solar wind and micrometeorite impact. An additional future production mechanism would be through the operations of man (drilling, coring, sample taking, experiment implacement, locomotion, etc.).

The studies conducted in this program have involved measurement between surfaces formed in air, and between surfaces formed in vacuum. The air-formed surfaces initially have their charge and coordination demands satisfied. Exposure to ultrahigh vacuum suffices to remove gross surface contamination, but it is likely that the surface demands remain to a large degree satisfied. These studies, hence, are representative of the possible lower bound lunar adhesion case. The vacuum formed (cleaved) surfaces represent, on the other hand, a possible upper bound for lunar adhesion (excluding time in contact effects). For these surfaces, the charge and coordination demands

are initially unsatisfied, and no contamination is present.

6.0 PREVIOUS RELATED WORK

The earliest work involving direct measurement of solid-solid silicate adhesion appears to be that of Tomlinson [1928, 1930] and of Stone [1930]. Tomlinson measured adhesion between glass and quartz (not strictly, at least historically, a silicate) balls and fibers, detecting adhesion forces between the balls as large as 10^3 dynes. Tomlinson's results, and particularly his interpretations of the adhesion as being atomic, were challenged by Stone, but apparently no satisfactory resolution of their differences was achieved. It should be noted, however, that the work was done in air, and even though careful cleaning techniques were used, a reasonably large amount of surface contamination, particularly adsorbed water, was undoubtedly present. Harper [1955] performed adhesion experiments with quartz spheres in air, finding adhesion forces as large as 1.5×10^2 dynes. Though he presented convincing arguments that these forces were not due to surface charging, it is likely that at least a monolayer of adsorbed water was present, so that the degree to which the silicate atomic bonding forces were active is uncertain. Smith and Gussenhoven [1965], also studying quartz, concluded that the observed adhesion was due to dispersion forces.

Only in the last few years have experiments been performed in ultrahigh vacuum. These have demonstrated the presence of silicate adhesion. Salisbury et al. [1964] experimented with polycrystalline silicate powers at a vacuum in the mid 10^{-10} mm Hg range. They found adherence of the power grains (ϕ 5μ in diameter) and made a rough calculation that the adhesion force was 2 to 3×10^{-4} dyne. In these experiments no high-temperature or other (e.g., ionic-electronic)

outgassing was attempted, and the adhesion was that under essentially zero prior load. This work was followed by that of Stein and Johnson [1964], who studied larger grains (up to 140μ in diameter) at pressures of 6×10^{-10} to 1×10^{-9} mm Hg with 1 day outgassing at about 100°C. They found that the force of adhesion (with no prior loading) increased with particle size, being in excess of 3×10^{-2} dyne for the larger particles. They noted that if prior loading had been used the adhesion force might have been significantly greater. Neither Salisbury et al. nor Stein and Johnson determined the nature of the force acting; they noted only that it was not due to surface charging but could be dispersion or normal atomic bonding forces.

Additional experiments on powders have been performed by Halajian (1964), Johnson and Greiner (1965), Bell (1966), and Blum et al. (1967). Halajian used powders of about 40μ in diameter. The pressures obtained were in the high 10^{-10} mm Hg range, and the system was maintained continuously at 200°C. The adhesion force, calculated from Halajian's results by Salisbury's method, is at least 3×10^{-2} dyne. Johnson and Greiner utilized powders of various grain sizes. They concluded that dispersion forces were probably responsible for most of the observed adhesion but that surface electrostatic charging also had an effect. Bell ground olivine at an ambient pressure of 2×10^{-7} mm Hg finding considerable sticking of the resulting powder to itself and the container. Bell, however, did not attempt to determine the nature of the adhesion forces. Finally, Blum et al. ground basalt at ambient pressures of 10^{-8} to 10^{-9} mm Hg finding adhesion of the powder to itself, unground rock and metal in the vicinity.

7.0 SAMPLE CHOICE AND PREPARATION

7.1 Sample Choice

a. Silicates

Five criteria were used in the choice of the silicate samples. These were first, that the samples be representative of the more commonly occurring igneous rock and meteorite silicate minerals; second, that in so far as possible the mineral suite should encompass the igneous rock range of acidic to ultrabacic (which includes the meteorites); third, that each sample be as perfect (as regards competency, purity) an example of the chosen mineral as can be obtained; fourth; that in so far as possible at least one example of each important crystal class be studied; and finally, that the sample physical properties be such that the sample can withstand the forming operations required in sample preparation.

A set of minerals which appeared to satisfy these criteria to a reasonably good degree were chosen. These were: orthoclase, microcline, albite, bytownite, labradorite, and andesine representing the feldspars; and hornblende, augite, and hypersthene representing the amphibole and pyroxene groups. Also, a tektite (Indochinite) and obsidian were picked for study since they represent disordered silicate structures.

Sample identity was checked by standard mineralogical techniques.

b Non-Silicates

The engineering samples used were chosen on the basis of 1) the materials might be used on lunar missions and exposed to the lunar surface environment

and/or 2) the materials provided interesting cases for study to better understand the mechanics of adhesion. The samples chosen for study were: spectroscopically pure aluminum, nickel and magnesium; commercially pure beryllium; titanium alloy (6Al, 4V); Al (2024), magnesium alloy (AZ31B); alumina (Stupakoff #1530); and aluminosilicate glass (Corning #1723). The metals chosen range in hardness from very soft (Al, Mg) to very hard (Be), and from very ductile (Al, Mg) to quite brittle (Be). The ceramic and glass used were chosen solely because of their possible lunar applications.

Chemical analyses were performed on all samples.

7.2 Sample Preparation

7.2.1 Silicates and Non-Metallic Non-Silicates

The crystal axes for each crystalline sample were first determined by means of a petrographic microscope, and marked. Cylinders, 0.5 cm in diameter, were then cut ultrasonically. During cutting, the samples were so oriented that the face of interest for the adhesion studies was perpendicular to the axis of the cylinder.

a. Air-Formed Surfaces

Those samples whose surfaces were to be formed in air were then cleaved into disks 0.32 cm thick. Intersecting perpendicular holes were drilled ultrasonically, one along the axis of the disk and dead-ended beneath the surface to be contacted, the other, smaller-diameter hole extending through the disk parallel to the contact face. The samples were fastened to the experimental apparatus (Figure 1) by inserting a metal slug into the dead-ended hole and

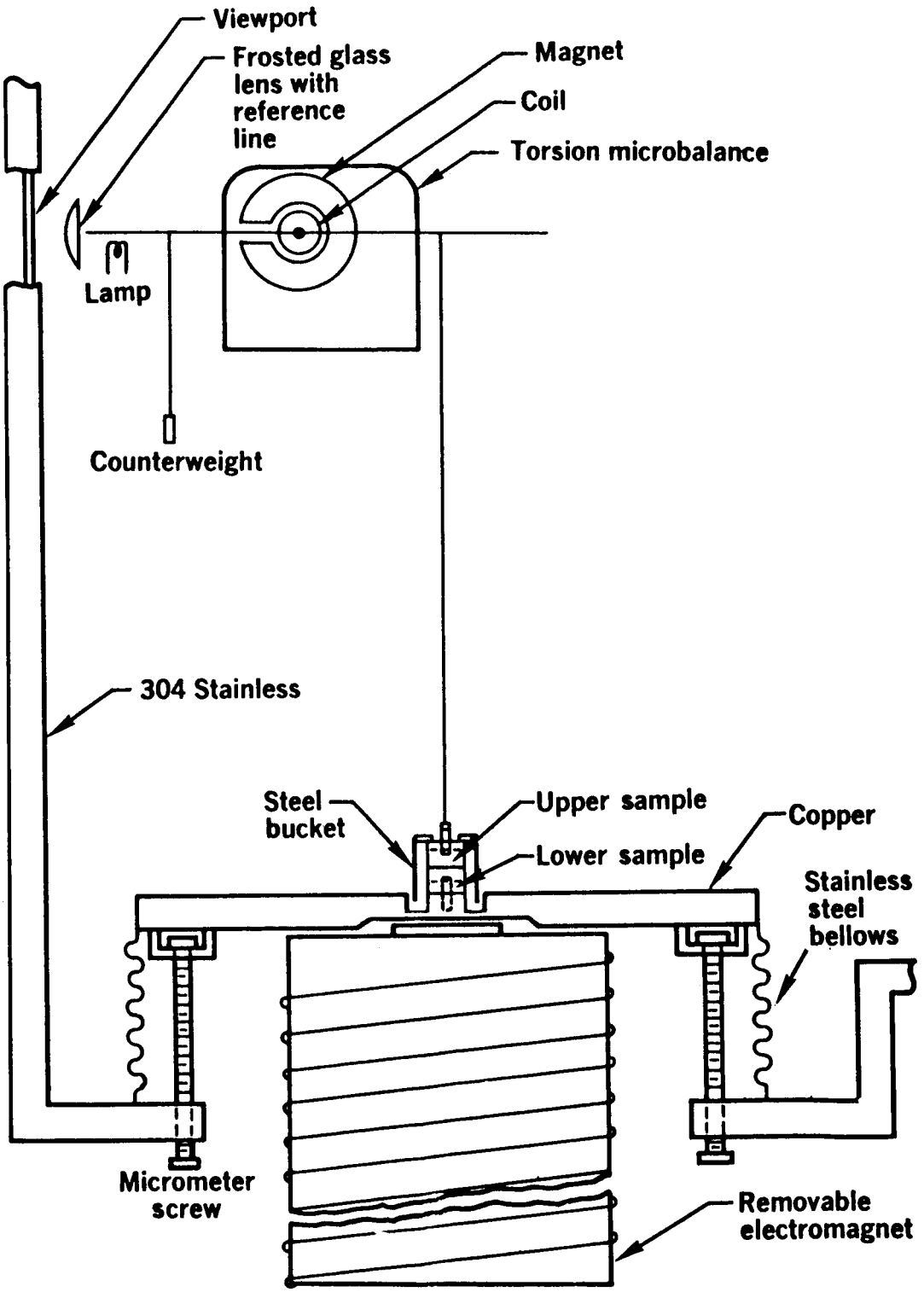

Figure 1. Exp. Apparatus for Studying Adhesion Between Air-Formed Surfaces

locking it with a fine wire inserted into the cross hole. The upper sample was attached to the adhesion-measuring device by inserting a wire through the exposed end of the slug. The lower sample was rigidly attached to the base plate by threading the slug into the base plate.

Each of the sample surfaces prepared in air was given a light (10-sec) etch with a mixture of approximately 30% (by volume) hydrofluoric acid, 30% glacial acetic acid, and 40% fuming nitric acid. The purpose of this etch was to remove surface dust contamination. The sample was immediately washed with distilled water and dried in an oven ($\approx 300°C$). The samples were then placed in the vacuum chamber and pumping was started.

Photomicrographs of the faces to be contacted were taken for all samples before and after each run, and surface roughness traces were made with a Bendix Proficorder. For most samples the peak-to-peak roughness averaged between 3 to 5μ; exceptions to this are noted later.

b. Vacuum-Formed Surfaces

All faces formed in vacuum were by cleavage, single or double. For single cleavage. the samples were formed into cylinders of diameter 0.5 cm and length 0.64 cm. They were notched ultrasonically at the desired cleavage plane. One pair of attachment holes was drilled (as for the air-formed case) to hold one end of the sample to the adhesion-measuring device, the other end being clamped to the base plate. For double cleavage, two samples were prepared, each 0.5 cm in diameter and 0.64 cm in length. A pair of attachment holes was drilled in the upper sample. The lower sample was clamped to the base plate and the two samples clamped together in-line. Both samples were notched at the desired cleavage planes.

7.2.2 Air-Formed Metals

All the metal samples were fabricated by standard machine shop techniques. All were disks, 0.5 cm in diameter and 0.32 cm thick. It was found necessary, due to the presence of undesirable ridges to give some of the samples a light polish with 3 micron aluminum oxide powder. All samples, immediately prior to use, were cleaned with detergent, rinsed then with water, cleaned again with trichlorethylene (electronic grade) followed by acetone (electronic grade) and deionized water. They were then oven dried and inserted into the vacuum system.

Photomicrographs of the faces to be contacted were taken prior to, and after, contact. Surface roughness traces were made with a Bendix Proficorder. The peak-to-peak roughness averaged between 3 and 10μ.

8.0 INSTRUMENTATION

8.1 Vacuum System

Runs during the first year of the program were made with a vacuum system consisting of a mechanical forepump with liquid nitrogen cold trap, a 200-l/sec ion pump, and the experimental chamber. The remainder of the runs in the series were made with a bank of sorption pumps replacing the mechanical pump. The purpose of this change was to determine whether the type of forepump had any effect on the adhesion data obtained. No effect was detected.

Pressure was monitored by a "nude" Bayard-Alpert ionization gage. This gage was shielded from direct exposure to the sample surfaces. The experimental chamber and the ion pump were separated from the low-vacuum section by an ultrahigh-vacuum bakeable valve that was closed during operation of the ion

pump. The chamber itself consisted of a 6-inch (diameter) tee and a 6-inch cross upon which was mounted the adhesion-measuring system. The vacuum seals were copper and gold gaskets.

Because of restrictions imposed by the adhesion-measuring device, system bakeout was limited to about 110°C. The bakeable valve was closed during all bakeouts. After each run the system was filled with nitrogen obtained from the top of a large liquid nitrogen tank. The lines leading from this tank to the vacuum chamber were flushed (with nitrogen from the tank) immediately before each filling. Since vibration interferes with adhesion studies, the entire ultrahigh vacuum section of the system was suspended from "soft" springs. With these springs the natural frequency of the suspended system, in its three oscillation modes was about 0.5 cps. This degree of isolation was found to be sufficient.

A base pressure of $1 - 4 \times 10^{-10}$ mm Hg was achieved in most instances with all the required equipment in the chamber.

8.2 Load Application System

An electromagnet, Figure 1, was used to apply load force (up to 10^6 dynes) to the samples for the study of the dependence of adhesion on load. A steel bucket was suspended from the upper sample. Passing current through the magnet attracted the bucket downward, hence applying load force. The current was then reduced to zero and the magnet withdrawn. A number of calibrations of load force as a function of current were made in the vacuum system at atmospheric pressure and utilizing Chatillion precision mechanical springs. The calibrations did not vary appreciably (< 10% for low current to <2% for maximum current).

This procedure worked well for the study of adhesion between air-formed surfaces since for these the surface gemetry could be controlled sufficiently to allow the required system stability to be achieved. However, it did not work for the vacuum cleaved surfaces since it was found to be difficult to produce sufficient surface flatness even for minerals supposedly possessing "perfect" cleavage planes. A load cell device was constructed to overcome this difficulty, but was not completed in time for data to be obtained.

8.3 Adhesion Measuring System

8.3.1 Adhesion of Air-Formed Surfaces

A Cahn torsion microbalance, Figure 1, measured adhesion force. Current passed through the meter movement coil (suspended in a magnetic field) applied torque to the balance arm, which along with the coil was supported by an elastic metal fiber. The adhesion force was measured as the current which must be passed through the coil to cause separation of the samples. Separation was detected by movement of the microbalance beam from the zero reference line and by observing the contacting surfaces with a cathetometer. The microbalance itself was attached to a linear motion feedthrough with which the balance (and upper sample) could be raised or lowered, bringing the samples into contact before the load force was applied and keeping them separated during bakeout. The minimum detectable adhesion force was about 2×10^{-2} dyne. The maximum measureable was 4×10^{2} dynes. The calibration techniques used were essentially the same as those recommended by the manufacturer.

8.3.2 Adhesion of Vacuum-Formed Surfaces

The adhesion force observed after vacuum cleavage was found to exceed, in magnitude, the pulling capacity of the microbalance ($> 0.4 \times 10^{2}$ dynes).

Accordingly, the microbalance was replaced by a precision mechanical spring attached to a linear motion feedthrough (Figure 2). Adhesion force was then determined by reading the spring deflection with a cathetometer as it was raised. The spring allowed measurement of adhesion force as small as 10^2 dynes and as large as 2×10^4 dynes.

8.4 Cleavage Devices

The cleavage device for the single cleavages is shown in Figure 2. It consisted of a wedge-shaped tool steel chisel and an anvil to provide support to the sample opposite the cleavage point. Cleavage was obtained by applying a gradually increasing pressure to the chisel (tip inserted in notch) until the sample halfs were wedged apart. Both the chisel and anvil were mounted on bellows to permit removal from the sample vicinity following cleavage.

The cleavage device for the double cleavages operated in the same manner. Here, however, two blades were used and the length of the anvil was extended to provide support opposite both cleavage planes. The anvil was also supplied with a clamp to hold the samples together prior to and during cleavage, and to remove the center section, composed of one half of each sample, after cleavage.

9.0 EXPERIMENTAL DATA

9.1 Adhesion Between Air-Formed Surfaces

9.1.1 Silicate-Silicate

The sample pairs used, along with pertinent comments about experimental conditions, are presented in Table 1.

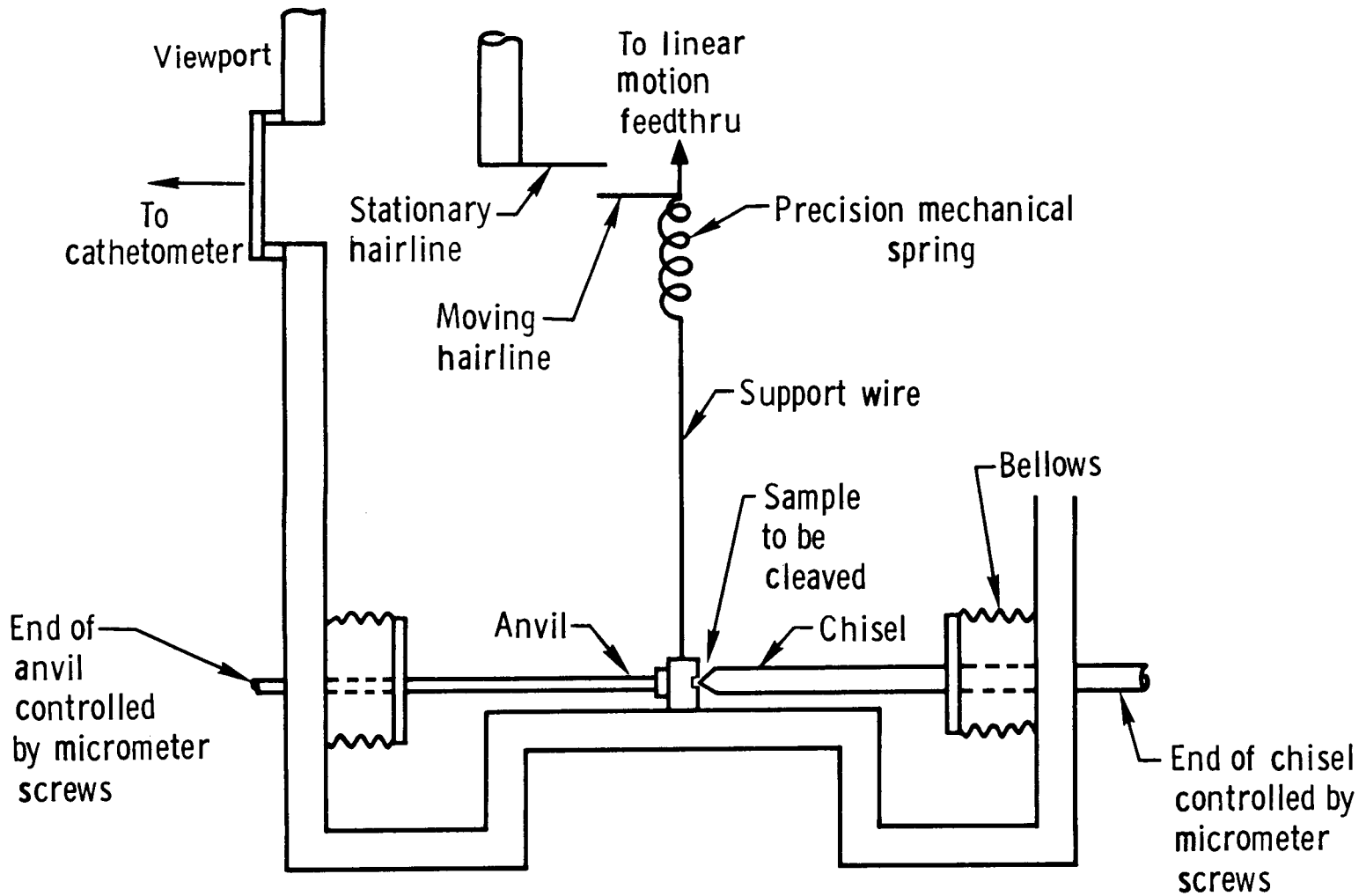

Figure 2. Exp. Apparatus for Studying Adhesion Between Vacuum-Cleaved Surfaces

TABLE 1. Experimental Conditions for Runs Involving Silicate Samples Formed in Air

Run No.	Upper Sample	Lower Sample	Orientation	Pressure, mm Hg	Forepump Type	Surface Roughness
1	Orthoclase (001)	Orthoclase (001)	α-Axis/α-Axis ≅ 10°	2-3 x 10^{-10}	Mechanical	4μ p.t.p., 10-μ hump, center of one sample
2	Orthoclase (001)	Orthoclase (001)	α-Axis/α-Axis ≅ 80°	4 x 10^{-10}	Mechanical	≈5μ p.t.p.
3	Hypersthene (110)	Orthoclase (001)	α-Axis trace/ α-Axis ≅ 10°	3 x 10^{-10}	Mechanical	≈5μ p.t.p.
4	Hypersthene (110)	Orthoclase (001)	α-Axis trace/ α-Axis ≅ 25°	1 x 10^{-10}	Sorption	≈3μ p.t.p.
5	Hornblende (101)	Bytownite (001)	α-Axis trace/ α-Axis ≅ 30°	3 x 10^{-10}	Mechanical	≈3μ p.t.p., 10 μ depression, center of one sample
6	Hornblende (101)	Bytownite (001)	α-Axis trace/ α-Axis ≅ 20°	1 x 10^{-10}	Sorption	≈5μ p.t.p.
7	Albite (001)	Orthoclase (001)	α-Axis/α-Axis ≅ 10°	3 x 10^{-10}	Mechanical	≈3μ p.t.p.

TABLE 1. Experimental Conditions for Runs Involving Silicate Samples Formed in Air (Continued)

Run No.	Upper Sample	Lower Sample	Orientation	Pressure, mm Hg	Forepump Type	Surface Roughness
8	Albite (001)	Orthoclase (001)	α-Axis/α-Axis ≅ 25°	2×10^{-10}	Sorption	≈3μ p.t.p.
9	Tektite	Tektite		2×10^{-10}	Mechanical	≈3μ p.t.p., measured on plate from which cut
10	Obsidian	Obsidian		6×10^{-10}	Mechanical	≈2μ p.t.p.
11	Orthoclase (001)	Orthoclase (001)	α-Axis/α-Axis ≅ 100°	4×10^{-10}	Sorption	≈0.5μ p.t.p.
12	Orthoclase (001)	Orthoclase (001)	α-Axis/α-Axis ≅ 90°	3×10^{-10}	Sorption	≈0.03μ p.t.p.
13	Orthoclase (001)	Orthoclase (001)	α-Axis/α-Axis 150°	2×10^{-10}	Sorption	≈5μ p.t.p.
14	Orthoclase (001)	Orthoclase (001)	α-Axis/α-Axis ≅ 40°	2×10^{-10}	Mechanical	≈4μ p.t.p.
15	Orthoclase (001)	Orthoclase (001)	α-Axis/α-Axis ≅ 190°	4×10^{-10}	Sorption	≈0.5μ p.t.p.

Attempts were made, for a number of the runs, to detect adhesion before evacuating the chamber, but none was detected. Adhesion appeared, however, once the system pressure entered the low 10^{-10} mm Hg range. For some of the runs, the samples were then baked for about 1 hour at 500-600°C. During this time the system pressure rose into the 10^{-7} mm Hg range. After sample bakeout and return of the pressure to the low 10^{-10} mm Hg range, adhesion was again detected. The high-temperature bakeout was found to have no effect on the magnitude of the adhesion. It was noted that time of exposure to vacuum did cause a slight increase in the adhesion magnitude (typically 10-20%).

We attempted to determine whether any long range attractive forces were present, such as those produced by surface electrostatic charging. This was done by slowly bringing the samples toward contact by decreasing the microbalance current and observing the balance pointer for any indications of an apparent increase in sample weight. Sample separation was monitored with a cathetometer. Only on rare occasions were there any indications of long-range forces and the magnitude of these forces, when observed, was much too small to affect the adhesion.

The results obtained for adhesion force as a function of load force are shown in Figures 3-6.

During two of the runs (#2 and #5), measurements were made to determine whether the adhesion force was temperature dependent. The results of these runs are shown in Figure 7.

After each run the system was then brought up to atmospheric pressure with dry nitrogen. Attempts were made to detect adhesion, and it was found that

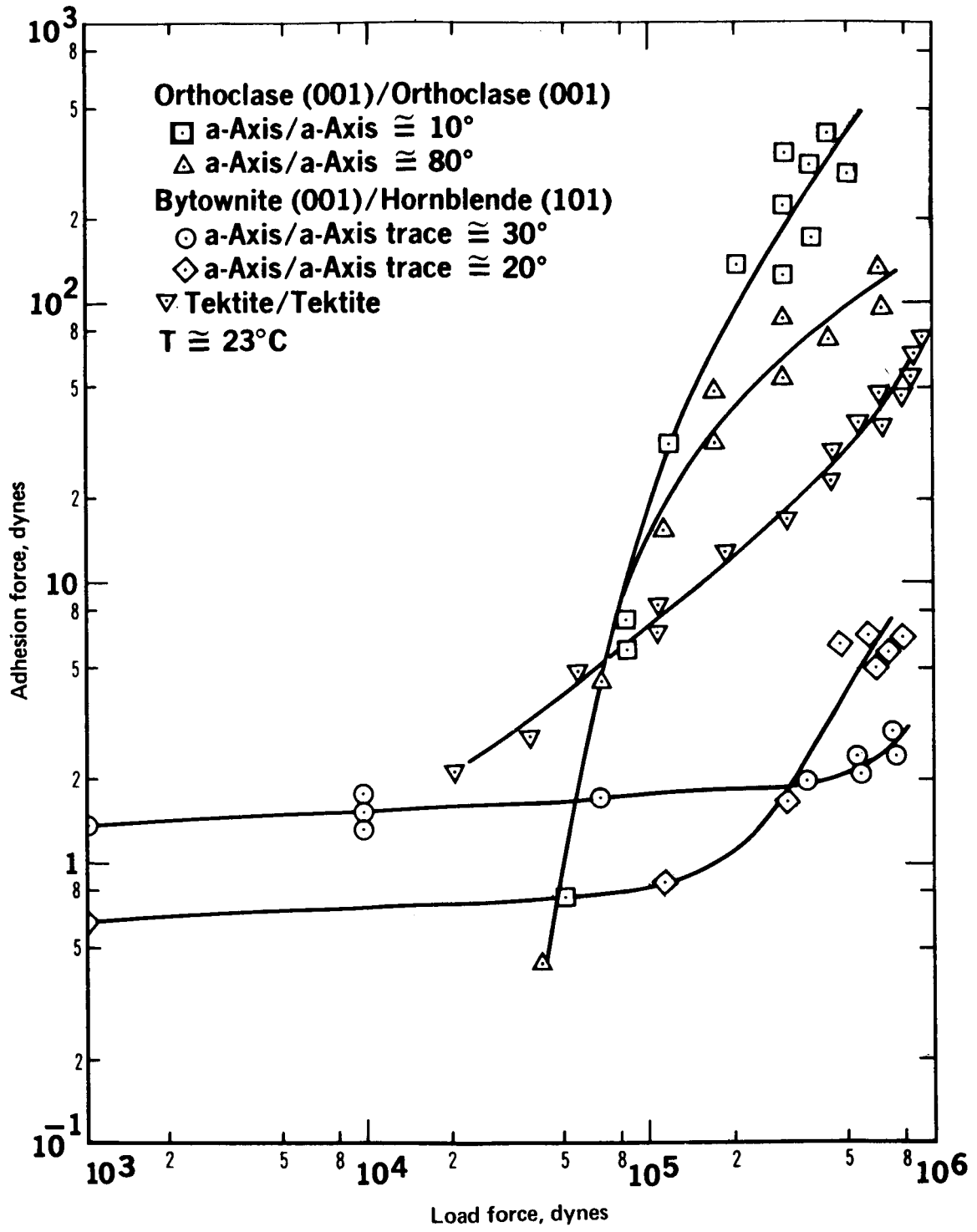

Figure 3. Adhesion Force vs Load Force for Various Air-Formed Silicates

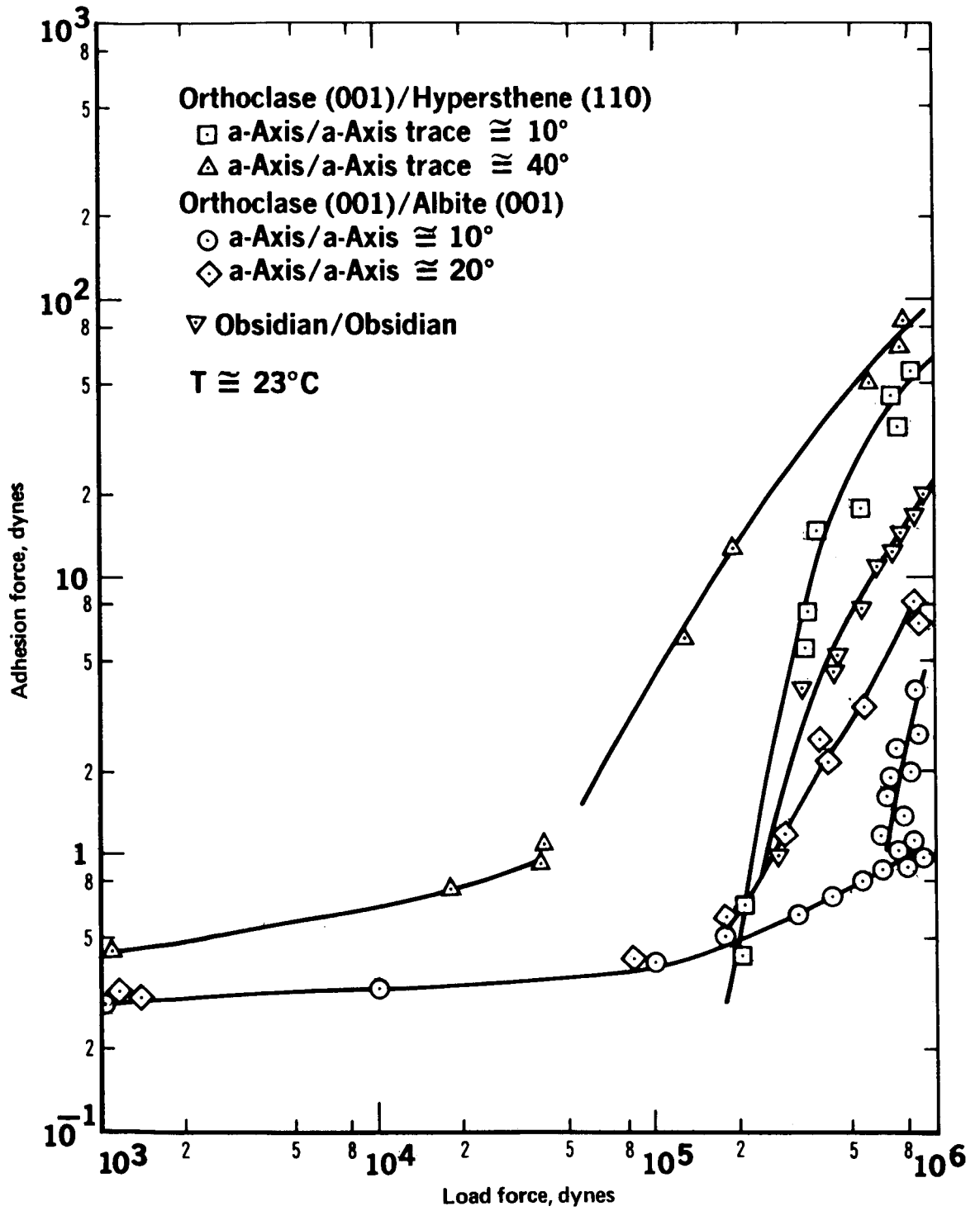

Figure 4. Adhesion Force vs Load Force for Various Air-Formed Silicates

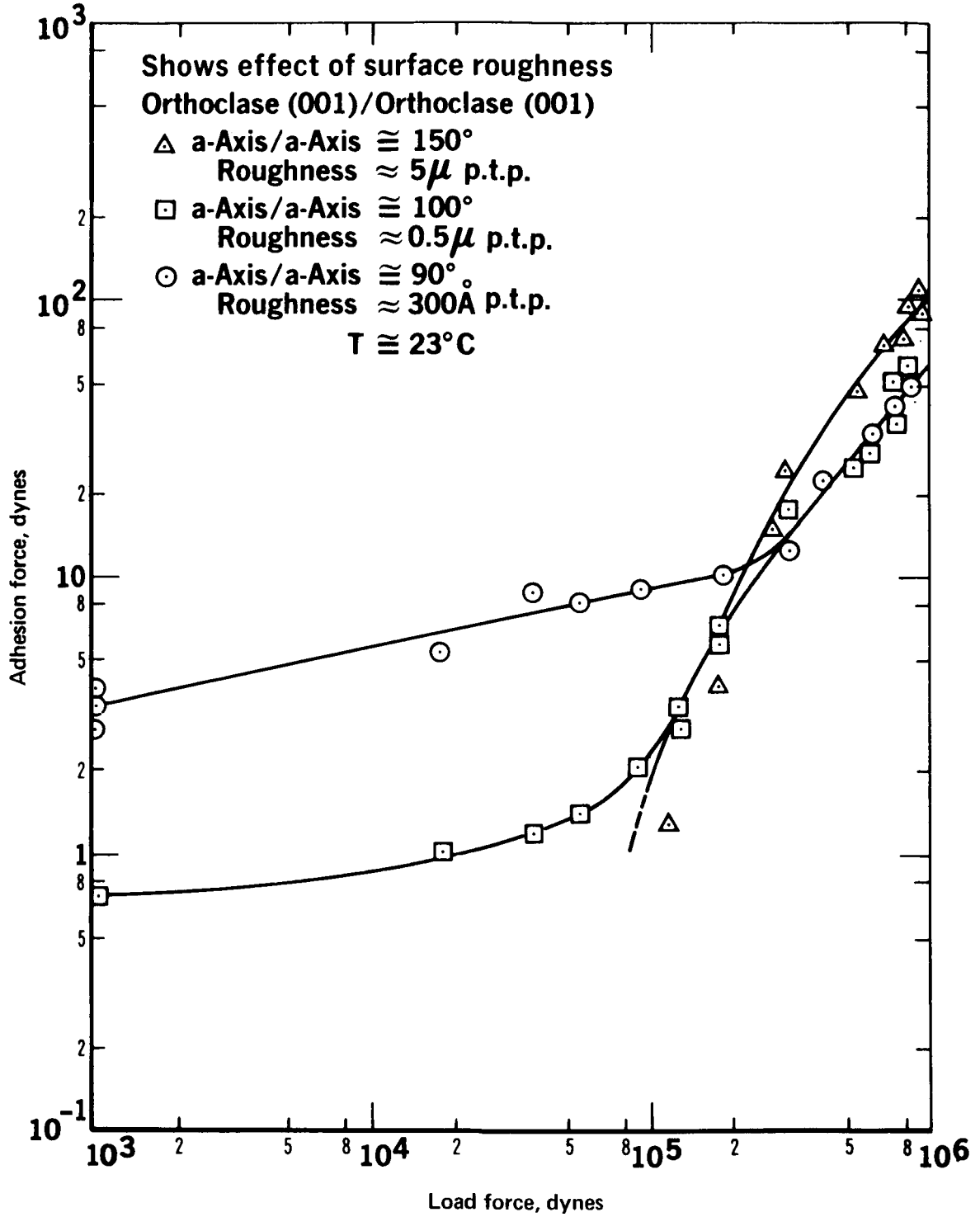

Figure 5. Adhesion Force vs Load Force for Various Air-Formed Silicates

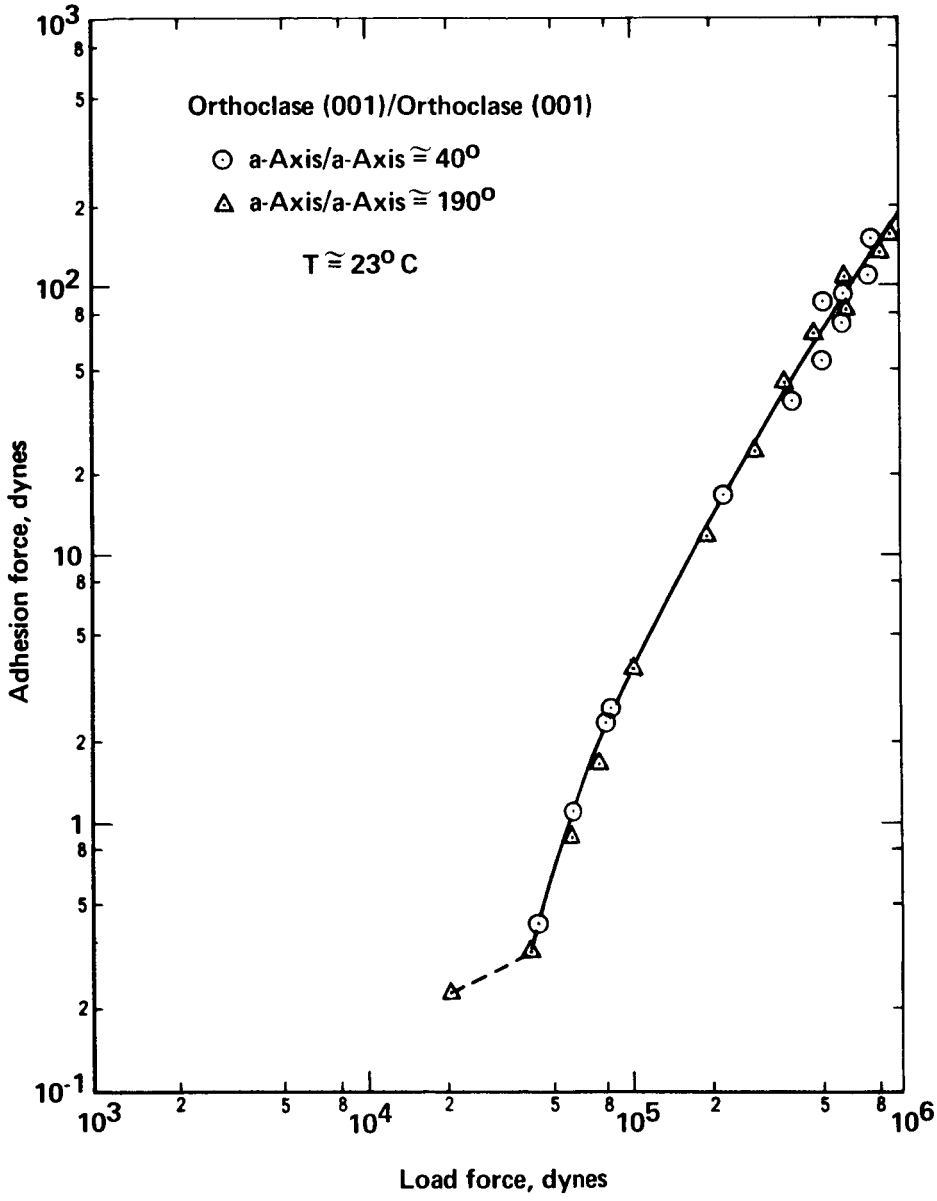

Figure 6. Adhesion Force vs Load Force for Various Air-Formed Silicates

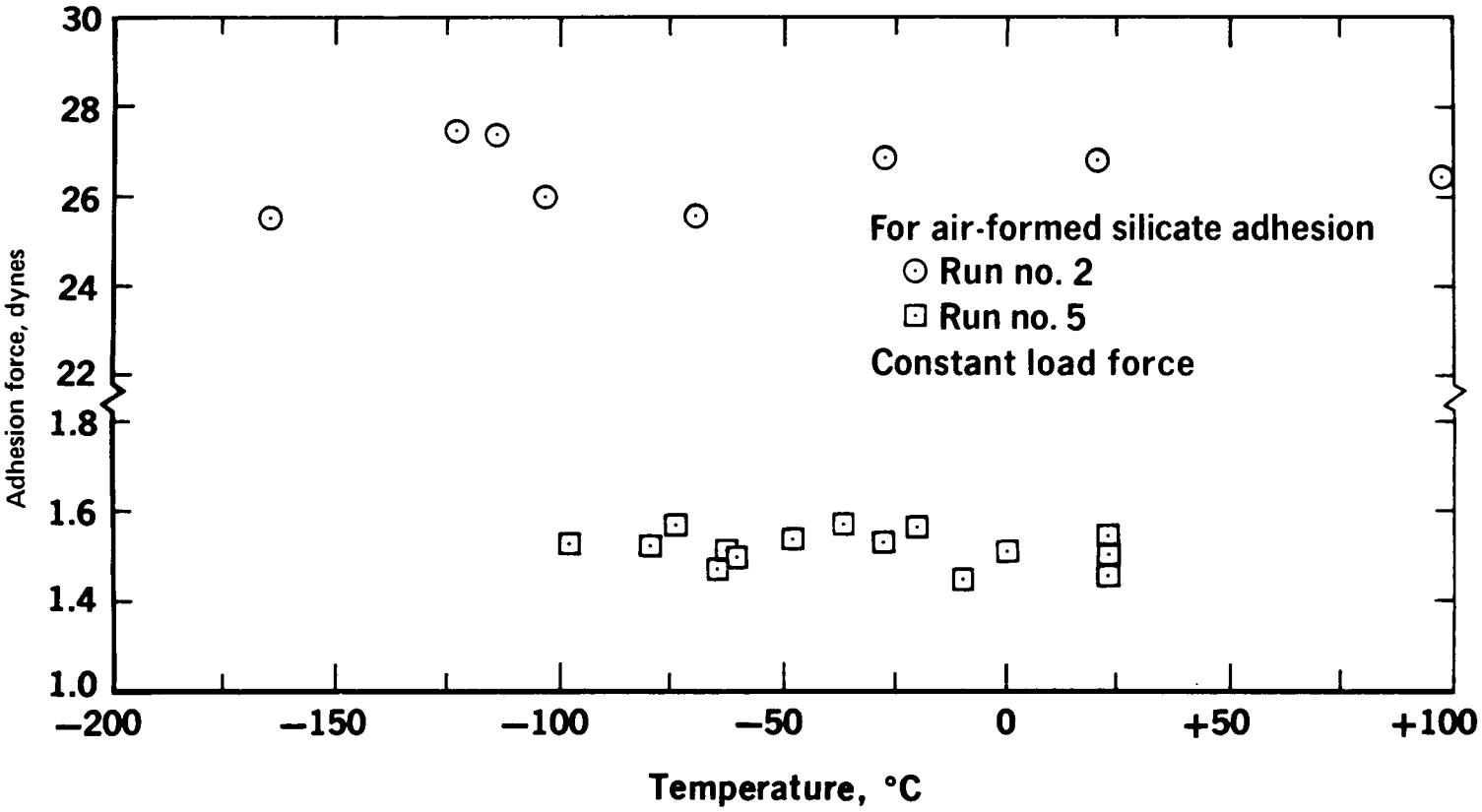

Figure 7. Adhesion Force vs Temperature, Runs no. 2 and 5

the higher magnitude adhesion had disappeared. However, the lesser magnitude adhesion produced under light load (that part in the figures showing only moderate load dependence) remained. Admittance of laboratory air to the system caused the immediate disappearance of all adhesion.

The sample contact faces were then studied with a Leitz petrographic (polarizing) microscope, and micrographs were taken.

9.1.2 Silicate - Non-Silicate

The sample pairs used, along with pertinent comments about experimental conditions, are presented in Table 2. The experimental procedure used, and results found,were similar to that for air-formed silicates contacting silicates. The data for adhesion force as a function of load force are presented in Figures 8-10.

9.2 Adhesion Between Vacuum Cleaved Surfaces

9.2.1 Single Cleavage

The single cleavage studies consisted of the use of a single silicate sample, cleaving it at ultrahigh vacuum, rotating one half with respect to the other, recontacting the two fresh surfaces, and thereafter measuring the adhesion force as a function of time after cleavage. The pertinent experimental conditions are given in Table 3. Sorption forepumps were used for all runs.

Details of the observations for each run are given below:

Run #1 Cleavage Along Orthoclase (001) Plane

Cleavage was performed at a system pressure of 2×10^{-10} mm Hg. Following cleavage the upper sample rotated 10°. The first measurement was made fifteen

TABLE 2 Experimental Conditions for Runs Involving Silicate and Non-Silicate Samples Formed in Air

Run No.	Upper Sample	Lower Sample	Orientation	Pressure mm Hg	Forepump Type	Surface Roughness
1	Orthoclase (001)	Spectro. Pure Al	NA	3×10^{-10}	Mechanical	≈3μ p.t.p. Oxide layer present
2	Orthoclase (001)	Spectro. Pure Mg	NA	$3\text{-}4 \times 10^{-10}$	Mechanical	≈4μ p.t.p. Oxide layer present
3	Orthoclase (001)	Comm. Pure Be	NA	3×10^{-10}	Mechanical	≈5μ p.t.p. Oxide layer present
4	Orthoclase (001)	Ti Alloy (6Al4V)	NA	3×10^{-10}	Mechanical	≈3μ p.t.p. Oxide layer present
5	Orthoclase (001)	Al Alloy (2024)	NA	2×10^{-10}	Sorption	≈0.6μ p.t.p. Oxide layer present
6	Orthoclase (001)	Mg Alloy (AZ31B)	NA	1×10^{-10}	Sorption	≈3μ p.t.p. orthoclase; 0.6μ p.t.p. magnesium. Oxide layer present
7	Orthoclase (001)	Spectro. Ni	NA	2×10^{-10}	Sorption	≈4μ p.t.p. orthoclase; ≈1μ p.t.p. nickel. Oxide layer present
8	Orthoclase (001)	Glass (Corning #1723)	NA	3×10^{-10}	Mechanical	≈5μ p.t.p. orthoclase; optical glass
9	Orthoclase (001)	Alumina (Stupakoff #1530)	NA	5×10^{-10}	Mechanical	≈5μ p.t.p.

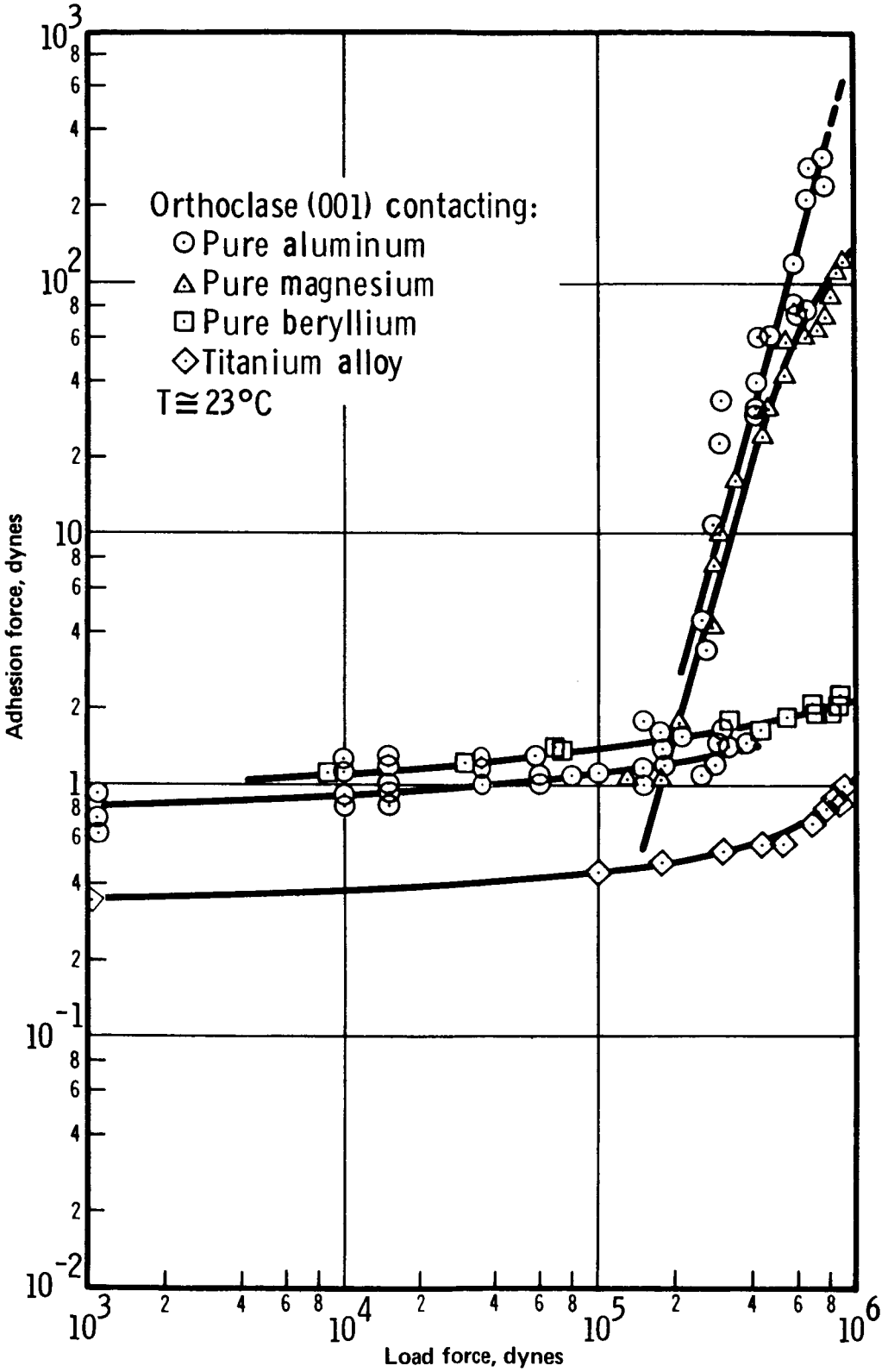

Figure 8. Adhesion Force vs Load Force for Various Metals (Metal Oxides) Contacting Silicates

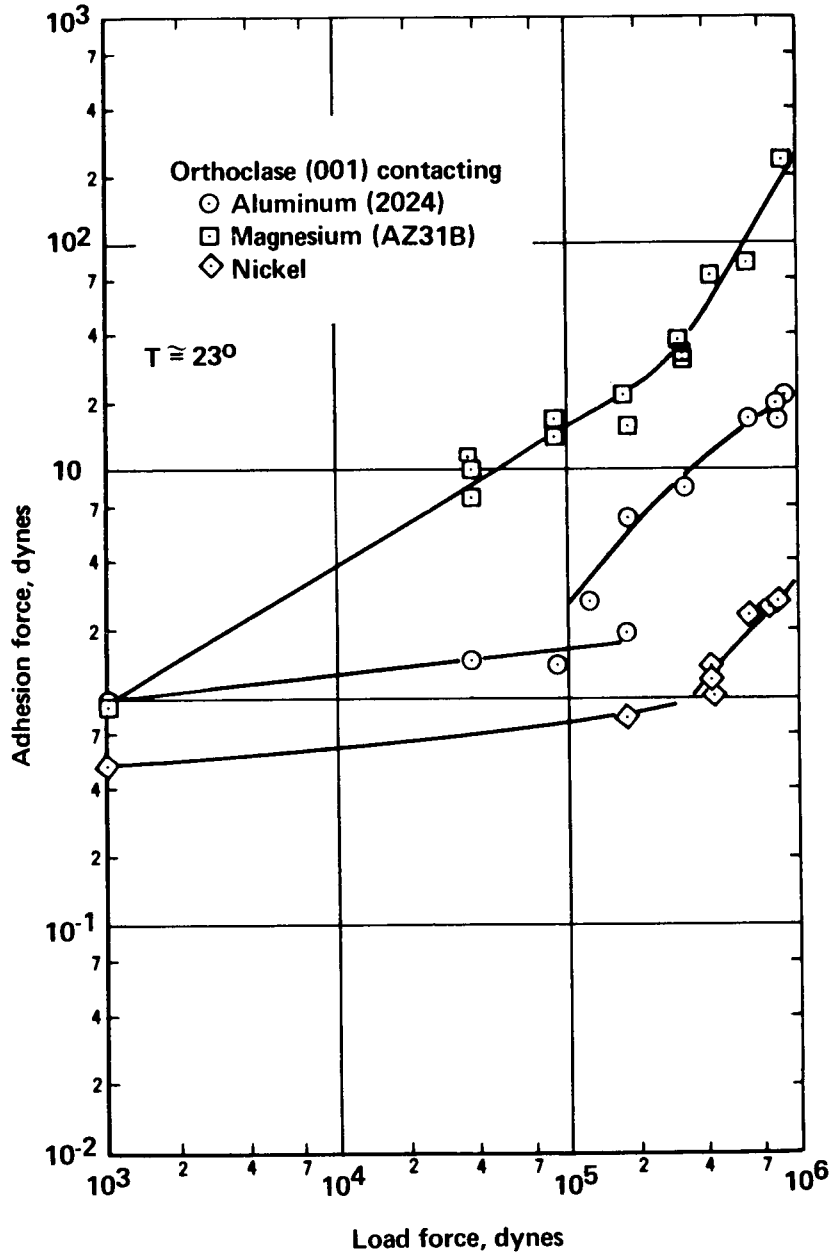

Figure 9. Adhesion Force vs Load Force for Various Metals (Metal Oxides) Contacting Silicates

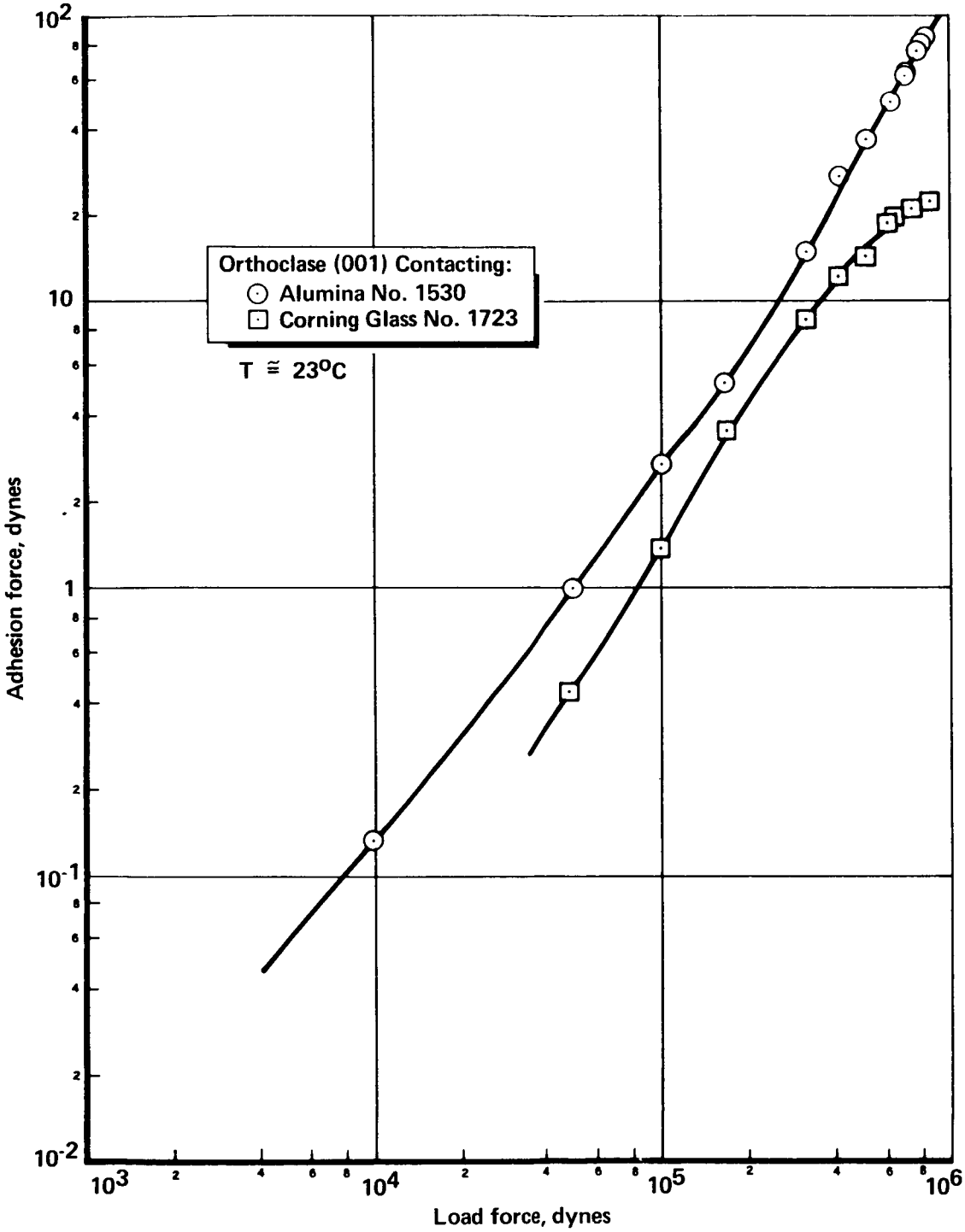

Figure 10. Adhesion Force vs Load Force for Glass and Ceramic Contacting Silicates

TABLE 3 Experimental Conditions for Single Ultrahigh Vacuum Cleavage Runs

Run No.	Sample	Cleavage Plane	Respective α-Axis Orientation	Pressure (mm Hg)	Comments
1	Orthoclase	(001)	10°	2×10^{-10}	No pressure burst
2	Labradorite	(001)	30°	1×10^{-10}	Cleavage surfaces quite rough. Pressure burst to 5×10^{-10} mm Hg.
3	Microcline	(001)	15°	2×10^{-10}	Contact copper baseplate. Pressure burst to 2×10^{-9} mm Hg.
4	Andesine	(001)	40°	3×10^{-10}	Cleavage surfaces quite irregular. Pressure burst to 1×10^{-9} mm Hg.
5	Labradorite	(001)	40°	2×10^{-10}	Cleavage surfaces very rough. Pressure burst to 4×10^{-9} mm Hg.
6	Labradorite	(001)	45°	2×10^{-10}	Pressure burst to mid 10^{-10} mm Hg range
7	Labradorite	(001)	45°	3×10^{-10}	Pressure burst to mid 10^{-10} mm Hg range
8	Labradorite	(001)	30°	2×10^{-10}	Pressure burst to 8×10^{-9} mm Hg
9	Orthoclase	(001)	5°	$1\text{-}2 \times 10^{-10}$	No pressure burst
10	Orthoclase	(001)	10°	$2\text{-}3 \times 10^{-10}$	Pressure burst to top of 10^{-10} mm Hg range
11	Orthoclase	(001)	10°	$1\text{-}2 \times 10^{-10}$	No pressure burst

minutes after cleavage. This gave a force of adhesion of 8×10^3 dynes. A strong long range attractive force was noted. This was sufficient to pull the samples together when separated by about 1 mm, giving a force of about 2×10^3 dynes. A second measurement of adhesion force was made five minutes after the first. This gave an adhesion force of 3×10^3 dynes, and a pull-down force again of 2×10^3 dynes. The third measurement gave a force of adhesion and pull-down force both of 2×10^3 dynes. Subsequent readings maintained this equivalence of forces. The system was kept at vacuum for 234 hours. During this time, the magnitude of the adhesion, and the long range force, decreased slowly to about 4×10^2 dynes. The data are plotted in Figure 11.

Upon admission of nitrogen to the system, all indications of adhesion immediately disappeared.

Run #2 Cleavage Along Labradorite (001) Plane

Cleavage was performed at a system pressure of 1×10^{-10} mm Hg. During cleavage, a pressure burst to 5×10^{-10} mm Hg was observed. After cleavage the upper sample rotated 30-40°. The cleavage surface was poor in that a number of noticeable steps were present with one relatively large prong sticking up from the edge of the lower sample. The samples were then brought into contact; the alignment was poor in that the upper sample was displaced from the lower sample with the apparent contact area being only about one fifth the total sample area. The first measurement of adhesion was made four minutes after cleavage and resulted in a force of 9×10^2 dynes. Only a slight indication of a long range force was detected, and its magnitude was slightly below measurement capability ($< 1 \times 10^2$ dynes). The alignment was

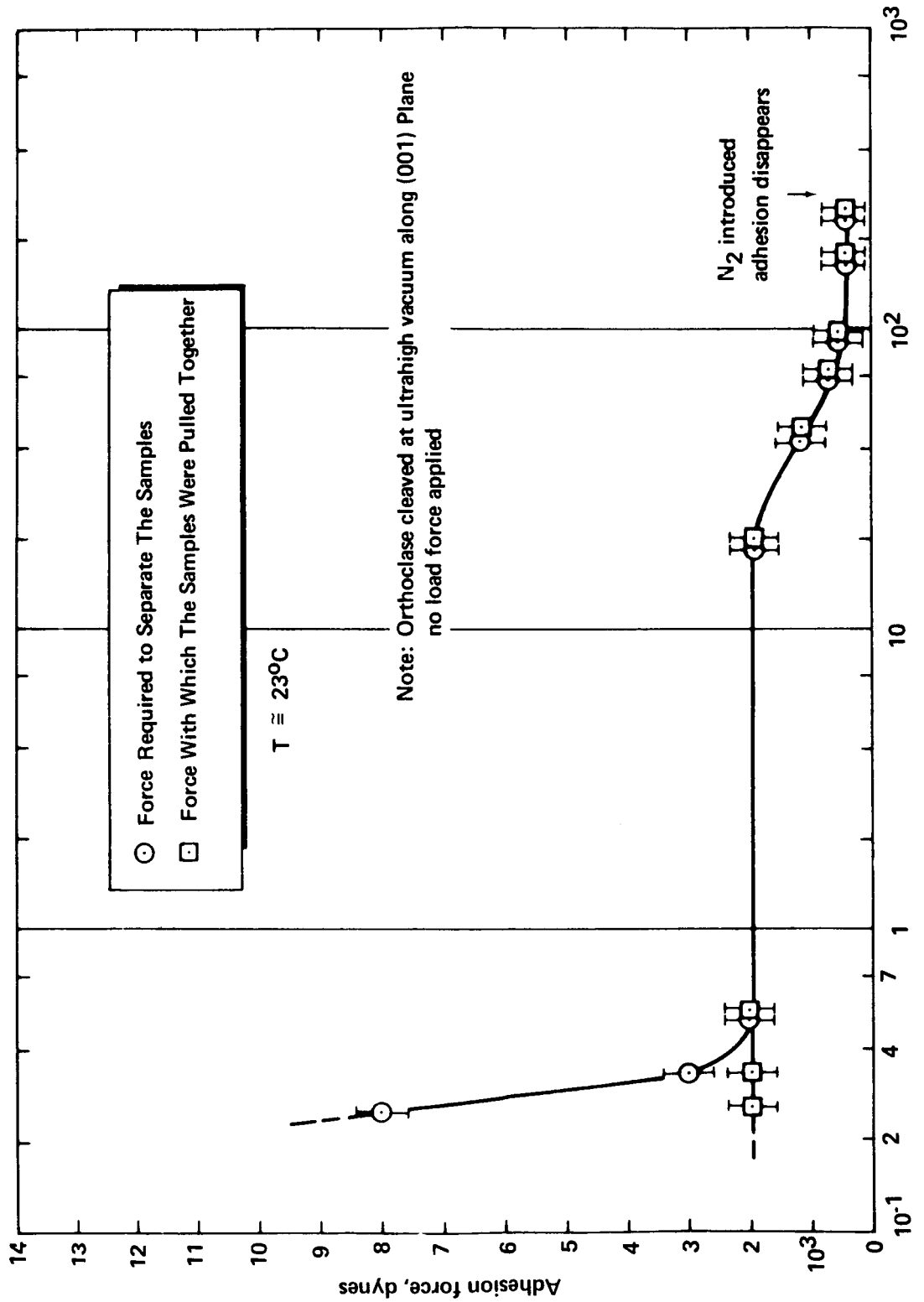

Figure 11. Adhesion Force vs Time, Run No. 1

then improved and further adhesion measurements were made. The adhesion force was found to decrease rapidly with time, leveling off at 4×10^2 dynes after about 10 minutes. Attempts were made to apply a load force in order to measure the load dependence of the adhesion. These attempts were unsuccessful due to the irregularity of the cleavage surfaces. The system was maintained at vacuum for 167 hours after cleavage during which time only a slight further decrease in adhesion magnitude occurred. All indications of adhesion disappeared upon admission of nitrogen to the system.

The data obtained are presented in Figure 12.

Run #3 Cleavage Along Microcline (001) Plane

Cleavage was made at a system pressure of 2×10^{-10} mm Hg. During cleavage, a pressure burst to 2×10^{-9} mm Hg was observed. After cleavage the upper sample rotated about 15°. Prior to recontact with the lower sample, the upper sample inadvertently contacted the copper base plate. It adhered strongly to this, but no measurement of the adhesion magnitude was obtained. First sample contact was made 20 minutes after cleavage. The adhesion force was 10^2 dynes, and there were no indications of a long range force. This adhesion remained constant over the next four hours, at which time the run was terminated. Microscopic studies showed the presence of copper flakes adhering to high spots on both samples.

Run #4 Cleavage Along Andesine (001) Plane

Cleavage was made at a system pressure of 3×10^{-10} mm Hg. During cleavage, a pressure burst to 1×10^{-1} mm Hg was observed. After cleavage the upper sample rotated about 40° and within one minute recontacted the lower sample.

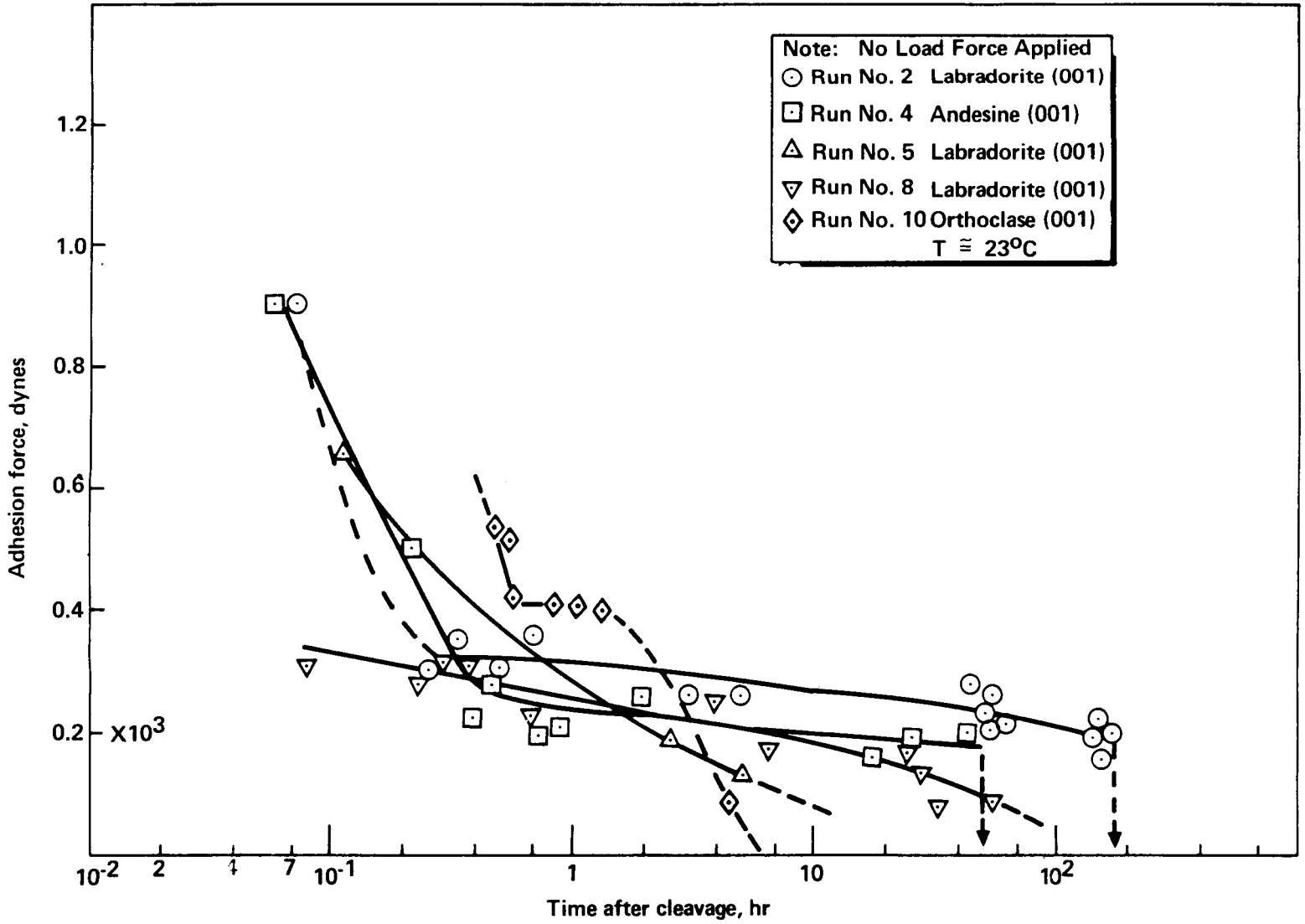

Figure 12. Adhesion Force vs Time for Various Silicates Cleaved at Ultrahigh Vacuum

The cleavage surfaces had several large steps on them so that contact was poor. The first measurement of adhesion gave an adhesion force of 9×10^2 dynes. The force decreased over the next 20 minutes to about 3×10^2 dynes. It thereafter decreased very slowly to a value of about 10^2 dynes over a period of 42 hours. Only very slight indications of a long range force were detected. All indications of adhesion disappeared upon admission of nitrogen to the system.

The data obtained are presented in Figure 12.

Run #5 Cleavage Along Labradorite (001) Plane

Cleavage was made at a system pressure of 2×10^{-10} mm Hg. During cleavage a pressure burst to 4×10^{-9} mm Hg was observed. After cleavage the upper sample rotated about 40° and recontacted the lower sample within one minute. The cleavage surfaces were the poorest of any produced to date, being very irregular and having more the appearance of fractured surfaces. Contact between the two surfaces was solely at a raised area near the center of the lower sample, and the surfaces over the greater part of their area were separated by several tenths of a millimeter. Initial measurement of adhesion, about 7 minutes after cleavage, gave an adhesion force of about 6×10^2 dynes. Only a very slight indication of a long range force was detected, and its magnitude was below measurement capability. The adhesion rapidly decreased to below detectable in about 40 minutes. During this time the cleavage device was brought into the vicinity of the upper sample to see whether the sample would be attracted to it. No attraction was noted.

The data obtained are presented in Figure 12.

Run #6 Cleavage Along Labradorite (001) Plane

Cleavage was made at a system pressure of 2×10^{-10} mm Hg. During cleavage a pressure burst to the mid 10^{-10} mm Hg range was observed. After cleavage the upper sample rotated about 45° and recontacted the lower sample within one minute. The first measurement of adhesion, made 18 minutes after cleavage, gave a force of 1.5×10^{3} dynes. This decreased to 10^{3} dynes after 8 minutes. The lower sample was then rotated so that it was about 5° from atomic match in orientation with the upper sample. The adhesion force immediately increased to about 2.8×10^{3} dynes. A distinct long range attractive force was noted, which was sufficiently strong to bring the samples into contact at separations less than about 1 mm. The chisel was brought to the upper sample; no attraction of the sample to the chisel was detected. It was also noted that for the 5° alignment the upper sample, as it approached the lower sample, would rotate into what appeared to be atomic match (0°) as it was pulled into contact.

The lower sample was then rotated into various positions of atomic mismatch in orientation and it was found that upon doing this, the magnitude of the adhesion force decreased somewhat, and no indication of a long range force could be detected. The samples were then rotated back to the 5° orientation and the resultant observations were the same as reported previously. The system was maintained at vacuum for about 330 hours after cleavage, during which time the adhesion force decreased slightly.

The data up to T = 330 hours are presented in Figure 13.

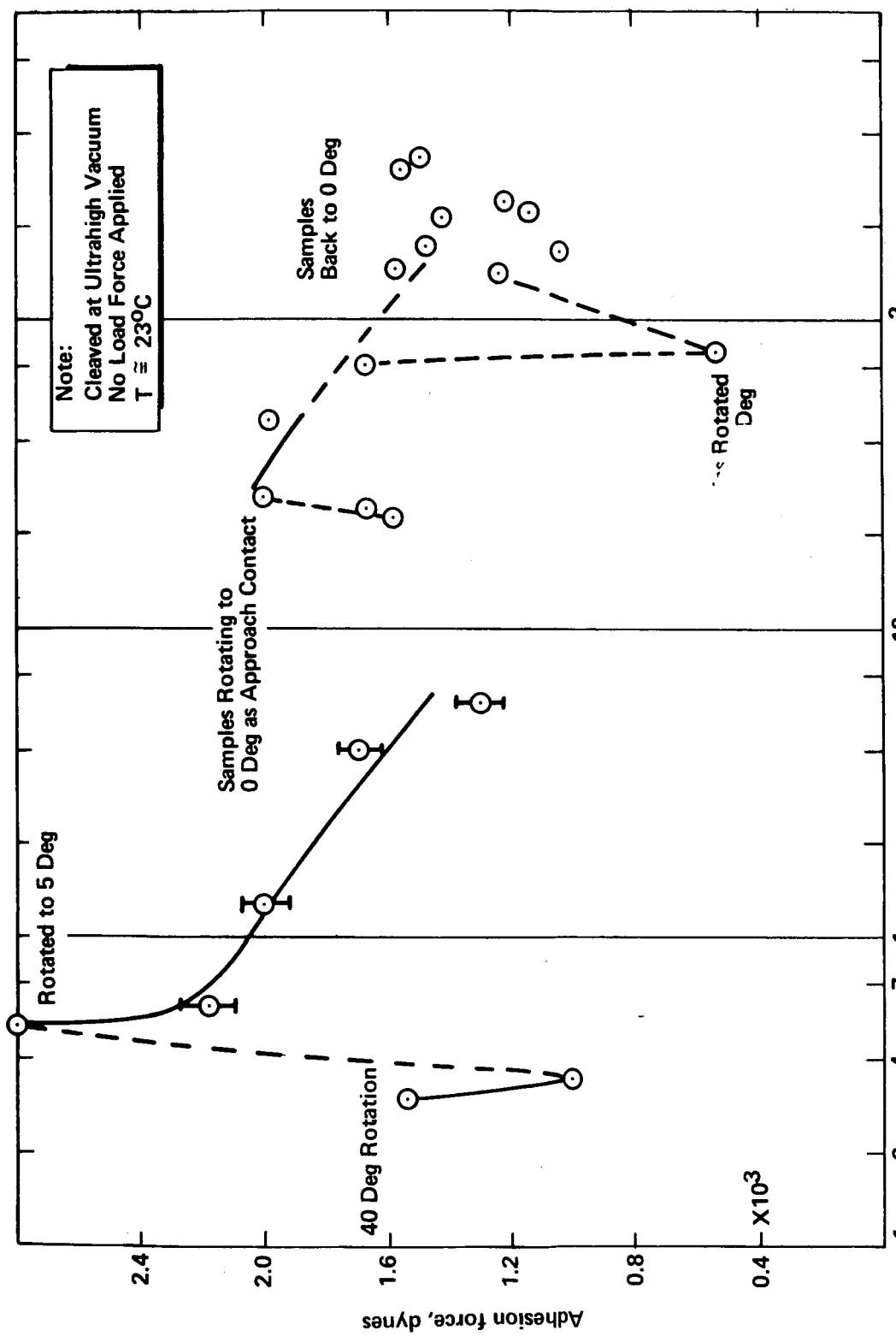

Figure 13. Adhesion Force vs Time and Orientation for Labradorite (001), Run No. 6

At T = 330 hours the ion pump was turned off, allowing the system pressure to rise slowly. In 30 minutes the pressure had risen to 9×10^{-9} mm Hg. The adhesion force was much smaller, as was the long range force. The pump was then turned on, the system pumped to 2×10^{-10}, and the adhesion measured. It was found that both the adhesion and long range force were still small. However, within 20 minutes the adhesion force had increased to its previous value, whereas the long range force remained small. The pump was then cycled a second time with similar results except that the adhesion did not recover. Finally, the pump was turned off again and small bursts of nitrogen were admitted to the system. Detectable, but small, adhesion remained to a pressure of 10^{-4} mm Hg. At this point the system was let up to atmospheric pressure and all indications of adhesion disappeared. The data obtained are presented in Figure 14.

Run #7 Cleavage Along Labradorite (001) Plane

Cleavage was made at a system pressure of 3×10^{-10} mm Hg. During cleavage, a pressure burst to the mid 10^{-10} mm Hg range was observed. Following cleavage the upper sample rotated about 45°. The first measurement was obtained about 12 minutes after cleavage; the adhesion force was about 8×10^{2} dynes. The next measurement was not made until 20 hours later due to experimental difficulties and the adhesion force was $2\text{-}3 \times 10^{2}$ dynes at that time. The force decreased slowly thereafter, falling below measurement capability after about 70 hours. Some indications of a very weak long range force were detected during the early stages of the run.

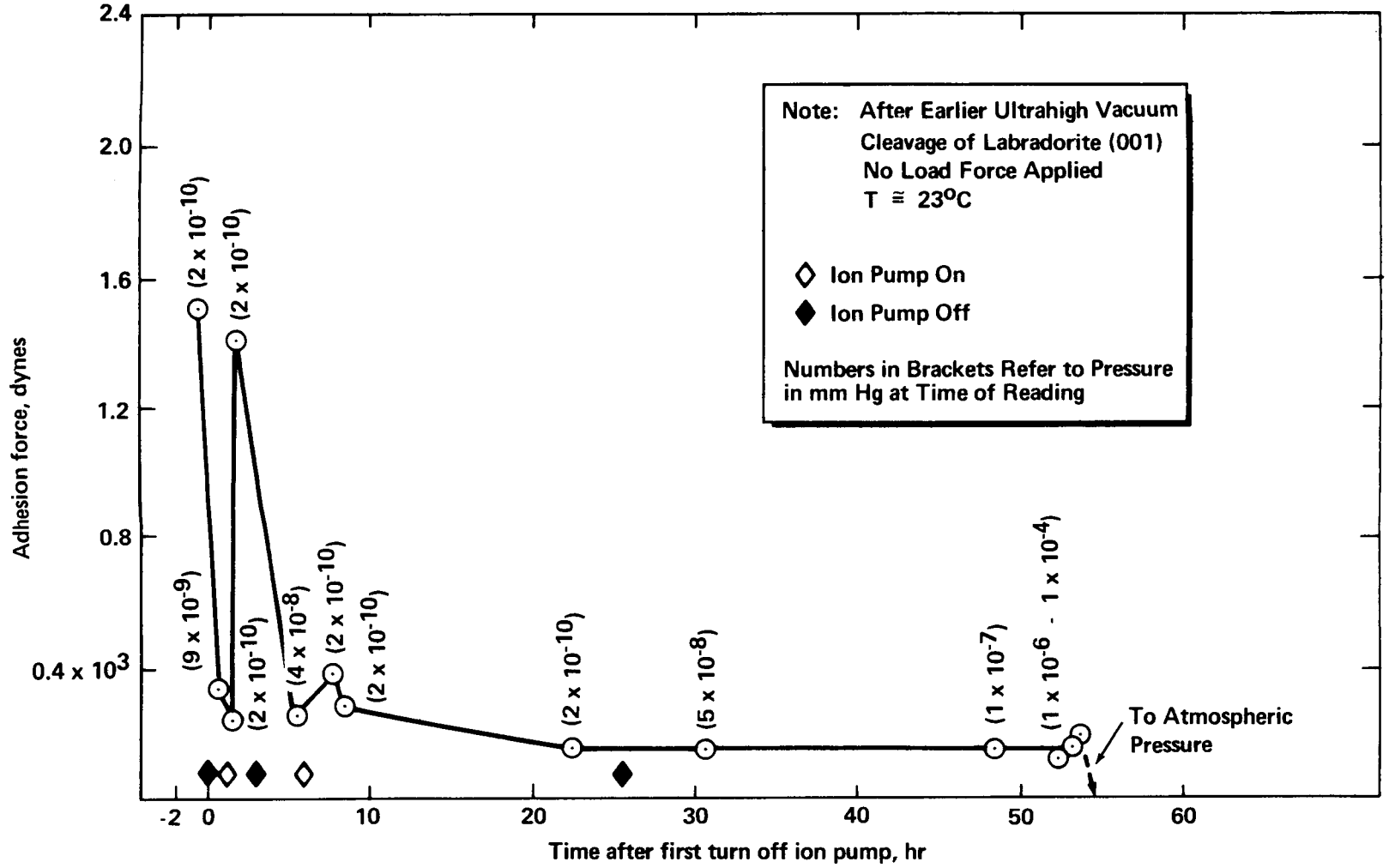

Figure 14. Adhesion Force vs System Pressure and Time, Run No. 6

Run #8 Cleavage Along Labradorite (001) Plane

Cleavage was made at a system pressure of 2×10^{-10} mm Hg. During cleavage, a pressure burst to 8×10^{-9} mm Hg was observed. Following cleavage the upper sample rotated about 30°. The first adhesion measurement was made 5 minutes after cleavage, giving a force of 3×10^{2} dynes. A significant long range force was present. The adhesion force decreased slowly to 10^{2} dynes over a period of 55 hours, at which time the experiment was terminated. The long range force remained moderately strong for about 1 hour after cleavage. Thereafter, it decreased rapidly to barely detectable. The data obtained are presented in Figure 12.

Run #9 Cleavage Along Orthoclase (001) Plane

Cleavage was performed at a system pressure of $1\text{-}2 \times 10^{-10}$ mm Hg. No pressure burst was observed. Following cleavage the upper sample rotated 5°. First contact occurred 3 min. after cleavage, resulting in an adhesion force of 1.1×10^{3} dynes. This force decreased slowly over the period of the experiment (while the pressure was maintained at $1\text{-}2 \times 10^{-10}$ mm Hg). The data are shown in Figure 15.

A long range attractive force was noted throughout this period. This force was initially sufficiently strong to bring the samples into contact at separations less than 1/4 to 1/2 mm. The magnitude of the adhesion force showed somewhat more variability than noted in previous runs. This appeared to be due to variations in sample alignment. The samples when apart were rotated a few degrees relative to each other, but if they were brought slowly toward contact the long range force field would rotate the upper sample into

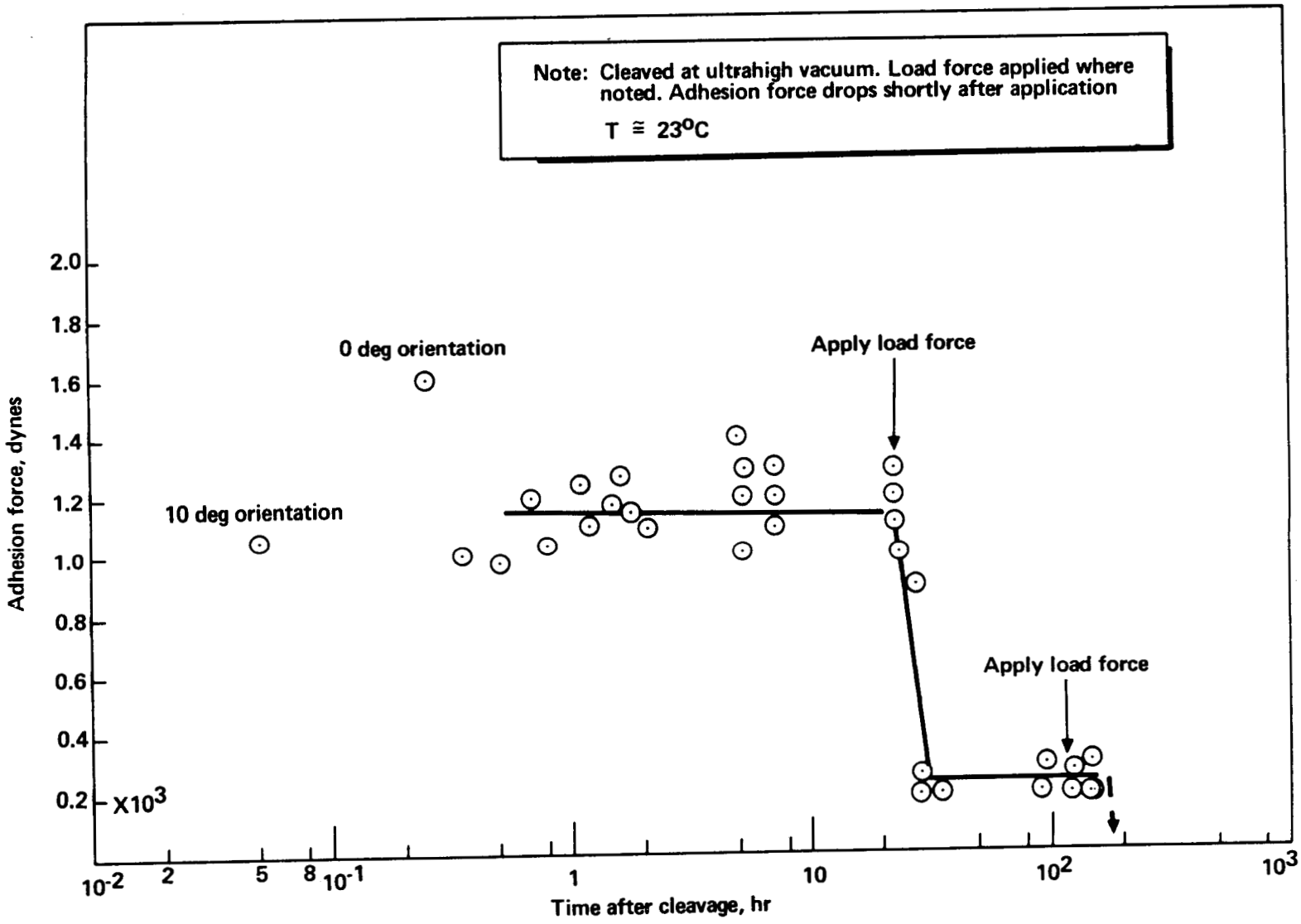

Figure 15. Adhesion Force vs Time and Orientation for Orthoclase (001), Run No. 9

what appeared to be atomic match with the lower sample. On the other hand, if the samples were brought together rather quickly some misalignment tended to remain. The measured adhesion force was largest when apparent perfect alignment was obtained, being in general about 30% - 40% smaller when some misalignment was evident. The data plotted in Figure 15 are for those measurements where to the best as could be observed perfect alignment had been achieved; it is seen that even for this case a significant amount of scatter remains. About 26 hours following cleavage, load forces (up to 8×10^5 dynes) were applied to the samples. No indications of a load dependence were obtained, but since difficulties were encountered in maintaining system stability nothing can be said as to whether or not a load dependence exists. Within two hours after the loadings were made it was found that an approximately 80% decrease in the adhesion force magnitude had occurred. It is not clear whether this decrease was caused by or related to the application of a load force to the surface. The new value of the adhesion ($2\text{-}3 \times 10^2$ dynes) remained constant thereafter, even though a second series of loadings was made about 100 hours after the first series.

The ion pump after about 144 hours at $1\text{-}2 \times 10^{-10}$ mm Hg was turned off. No change in the magnitude of the remaining adhesion was observed up to a pressure of 1×10^{-8} mm Hg, at which time the system was re-pumped to $1\text{-}2 \times 10^{-10}$ mm Hg. The pump was then again turned off and the bakeable valve opened slightly. The adhesion magnitude remained constant up to a pressure of 9×10^{-6}, and then all indications of adhesion rapidly disappeared. Evacuation of the system back to $1\text{-}2 \times 10^{-10}$ mm Hg did not restore the adhesion.

Run #10 Cleavage Along Orthoclase (001) Plane

Cleavage was performed at a system pressure of 2-3 x 10^{-10} mm Hg. During cleavage, a pressure burst to the top of the 10^{-10} mm Hg range was observed. The upper sample, after cleavage, was attracted to the metal anvil, and contacted it along one edge. The adhesion was strong, but it was not possible to obtain a measure of it. The upper sample rotated 10° with respect to the lower sample, and displaced laterally several millimeters. A relatively large adhesion force was evident, but due to the displacement no quantitative measurements of it were made until 25 minutes after cleavage. By this time it was readily evident that the adhesion had decreased by a significant amount. The first measurement, 25 minutes after cleavage, gave an adhesion force of 5 x 10^{2} dynes. Only a slight indication of a long range attractive force was detected. Also, there was no tendency for the samples to rotate into alignment. The adhesion decreased slowly over a period of 1 1/2 hours, and then rapidly disappeared in the course of an additional 3 1/2 hours. The data obtained are presented in Figure 12.

Run #11 Cleavage Along Orthoclase (001) Plane

Cleavage was performed at a system pressure of 1-2 x 10^{-10} mm Hg. No pressure burst was observed. After cleavage the upper sample rotated 10° and displaced laterally about 1 mm with respect to the lower sample. The first measurement of adhesion, obtained 4 min. after cleavage, gave an adhesion force of 1.2 x 10^{3} dynes. For this measurement the samples were 10° from match in rotation. A strong long range attractive force was noted. This was of sufficient strength to pull the samples into contact for separations less than 1 mm. For the second and subsequent contacts it was found that this long range force field was sufficiently strong (and anisotropic on a macroscale)

to rotate and displace the samples back to their pre-cleavage positions as they were brought toward each other. (As noted above these samples when out of contact were displaced laterally by about 1 mm and rotated 10°). The second adhesion measurement, at the 0° rotation and zero lateral displacement enforced by the long range attraction, gave a force of 1.7×10^3 dynes (larger than the first measurement). The adhesion then decreased slowly with time. No attraction of the upper sample to the chisel was detected.

After six hours with little change in the adhesion magnitude, the bottom sample was rotated so that it was about 30° out of atomic match in orientation with respect to the upper sample. As the samples were brought together the long range force again rotated the upper sample to 0° alignment and the adhesion force magnitude remained the same as before. The lower sample was then rotated so that it was 90° out of match. The long range force, as the samples were brought together rotated the upper sample so that when contact was made the samples were only 40° out of match. The resultant adhesion force dropped to 3×10^2 dynes. Next, the samples were rotated to 180° out of match. Unfortunately, in doing so flakes of metal from the chisel became deposited upon the face of the lower sample. These flakes prevented the two surfaces from coming into contact. When this occurred the adhesion force immediately dropped below measurement capabilities, as did the long range force. In order to make certain that this large decrease was not due to the 180° rotation, the samples were rotated back to 0°. The adhesion and long range force remained below measurement capabilities.

The data obtained are presented in Figure 16.

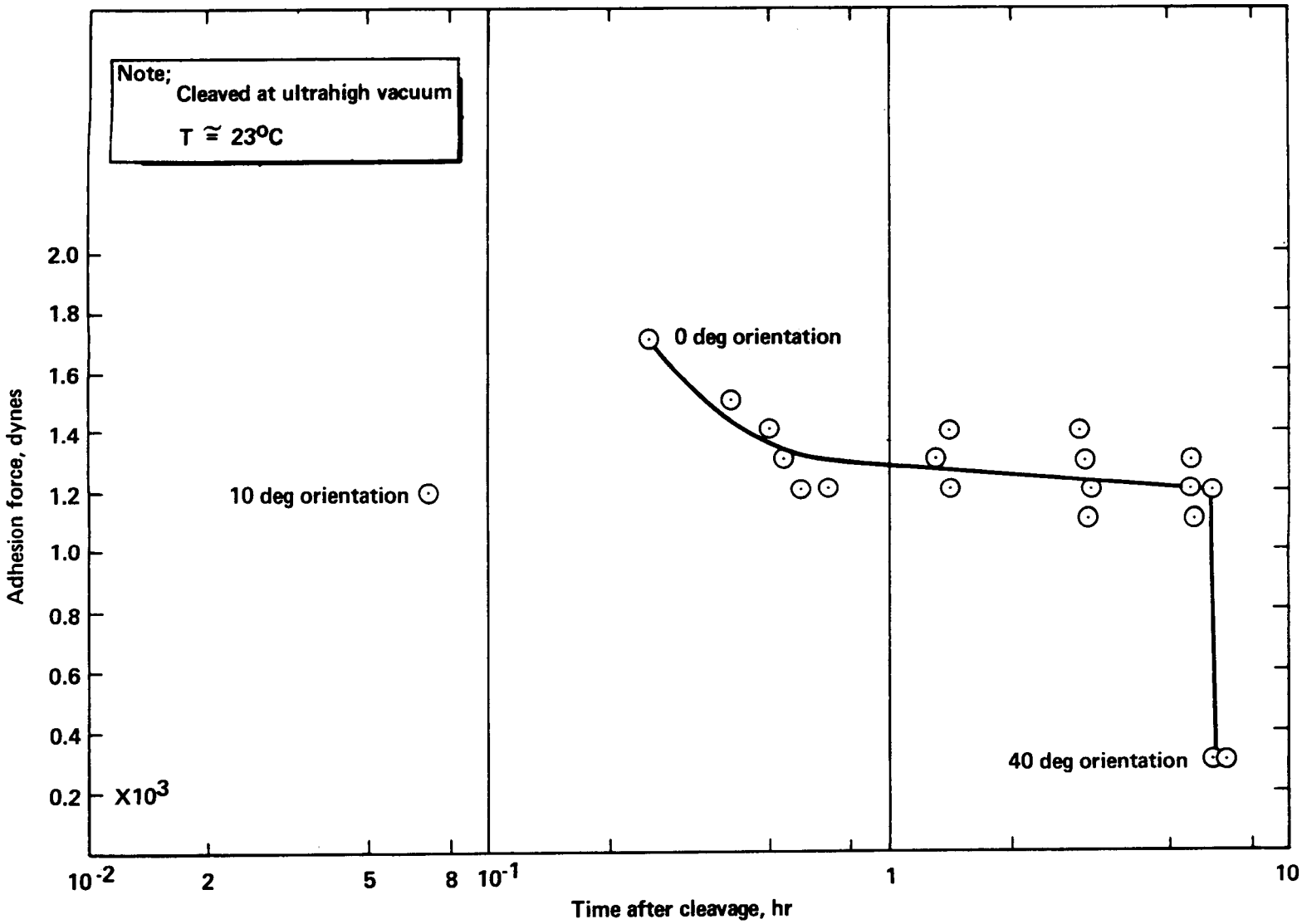

Figure 16. Adhesion Force vs Time and Orientation for Orthoclase (001), Run No. 11

9.2.2 Double Cleavage

The double cleavage studies consisted of the use of two silicate samples of, with one exception, differing composition and/or crystalline structure. Both samples were cleaved simultaneously, half of each sample removed from the experiment vicinity, the upper sample rotated, and then a fresh surface of sample A was contacted to a fresh surface of sample B. Adhesion force was measured as a function of time after cleavage. No load force was applied.

The pertinent experimental conditions are given in Table 4. Details of the observations for each run are given below.

Run #1 Orthoclase (001) and Microcline (001)

The double cleavage was performed at a system pressure of 2×10^{-10} mm Hg. A pressure burst to about 5×10^{-9} mm Hg was observed. During cleavage, the upper sample (microcline) broke not only at the desired spot but also at the cross-pin hole holding it to the mechanical spring. The lower sample broke into a number of pieces. As the upper sample was lowered, several chips of the fractured orthoclase attached themselves to the microcline fracture face. The largest chip was of dimensions about 0.5 x 0.5 x 1.0 mm. This attachment demonstrated the existence of adhesion and the indications were that a long range attractive force was present.

We were unable to remove the orthoclase chips from the microcline, but we were able with the chisel to move them over the surface to some degree. The particles remained attached until shortly after the system was brought to atmospheric pressure. At that time, all indications of adhesion disappeared.

Run #2 Orthoclase (001) and Microcline (001)

The double cleavage was performed at a system pressure of 2×10^{-10} mm Hg.

TABLE 4 Experimental Conditions for Double Ultrahigh Vacuum Cleavage Runs

Run No.	Samples	Cleavage Planes	Pressure (mm Hg)	Comments
1	Orthoclase Microcline	(001) (001)	2×10^{-10}	Pressure burst to 5×10^{-9} mm Hg Lower sample breaks into number of fragments
2	Orthoclase Microcline	(001) (001)	2×10^{-10}	Pressure burst to 5×10^{-9} mm Hg
3	Albite Labradorite	(001) (001)	3×10^{-10}	Pressure burst to 6×10^{-9} mm Hg Lower sample fractures
4	Orthoclase Microcline	(001) (001)	2×10^{-10}	Pressure burst to low 10^{-8} mm Hg range. Poor cleavages
5	Orthoclase Microcline	(001) (001)	2×10^{-10}	Pressure burst to top of 10^{-9} mm Hg range
6	Orthoclase Microcline	(001) (001)	3×10^{-10}	Pressure burst to top of 10^{-9} mm Hg range. No quantitative data
7	Labradorite Orthoclase	(001) (001)	4×10^{-10}	Pressure burst to mid 10^{-9} mm Hg range
8	Albite Orthoclase	(001) (001)	4×10^{-10}	Pressure burst to top of 10^{-9} mm Hg range
9	Orthoclase Orthoclase	(001) (001)	4×10^{-10}	Pressure burst to mid 10^{-9} mm Hg range

A pressure burst to about 5×10^{-9} mm Hg was observed. Both cleavages were good. No realignment of the samples occurred so that all contacts were made with the respective a-axes aligned. First contact was made five minutes after cleavage. This resulted in an adhesion force of about 4×10^{2} dynes. This force gradually decreased to below measurement capabilities in about two hours. The data are shown in Figure 17.

A long range attractive force was noted for all measurements. This force, however, did not give any indications of producing sample rotation or displacement. No sample repulsion was present at any time.

Run #3 Albite (001) and Labradorite (001)

The double cleavage was performed at a system pressure of 3×10^{-10} mm Hg. During cleavage, a pressure burst to 6×10^{-9} mm Hg was observed. The lower sample (labradorite) fractured at a large angle to the cleavage plane so that no quantitative data could be obtained. However, it was noted that several labradorite chips adhered to the upper (albite) sample.

Run #4 Orthoclase (001) and Microcline (001)

The double cleavage was performed at a system pressure of 2×10^{-10} mm Hg. During cleavage, a pressure burst to the low 10^{-8} mm Hg range occurred. Both cleavages were bad and a number of fragments were produced. A fragment of microcline adhering to the microcline (upper sample) was noted to jump to the lower sample as the samples were brought toward contact. Definite indications were observed for the presence of a long range attractive force between the samples. All indications of adhesion, however, disappeared before a measurement of adhesion magnitude could be made.

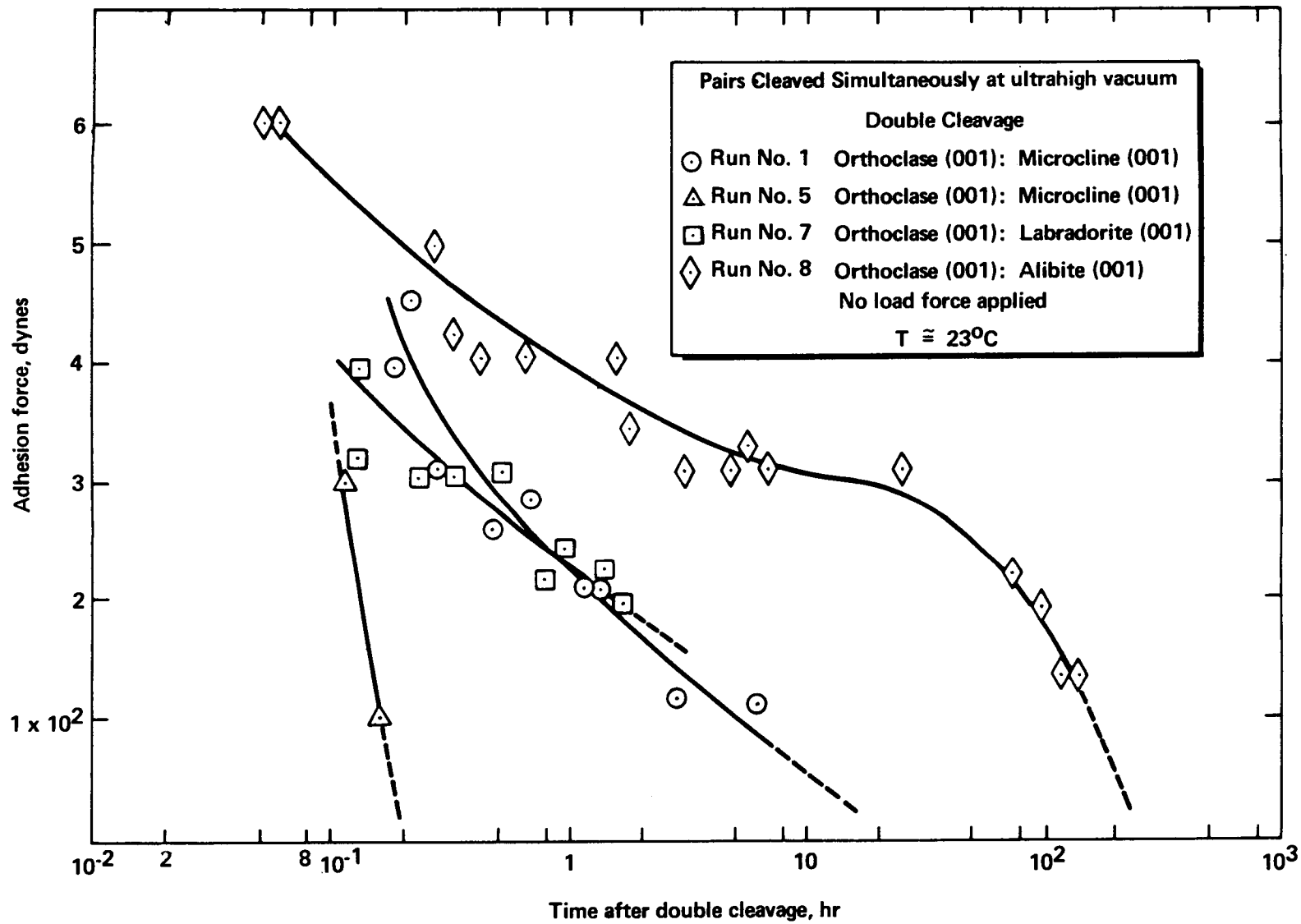

Figure 17. Adhesion Force vs Time for Various Sample Pairs

Run #5 Orthoclase (001) and Microcline (001)

The double cleavage was performed at a system pressure of 2×10^{-10} mm Hg. During cleavage, a pressure burst to the top of the 10^{-9} mm Hg range was observed. A long range attractive force was noted on bringing the samples toward contact. A small orthoclase chip on the orthoclase (bottom) sample was noticed to stand on end as contact was approached. This chip then stuck to the microcline. It was removed with the chisel. First contact, 6 minutes after cleavage, resulted in an adhesion force of 3×10^{2} dynes. This dropped to slightly below measurement ($< 10^{2}$ dynes) in two minutes. The data are shown in Figure 17.

Run #6 Orthoclase (001) and Microcline (001)

The double cleavage was performed at a system pressure of 3×10^{-10} mm Hg. During cleavage, a pressure burst to the top of the 10^{-9} mm Hg range was observed. Following cleavage, the upper sample (microcline) was attracted to the chisel and contacted it on one edge. The microcline was also attracted to the sample center sections during their removal. As the samples were brought toward contact several orthoclase chips ($\sim$ 1 mm long) stood on end, aligning themselves with the axis of the upper sample. One transferred to the microcline sample. These chips were then removed with the chisel. Due to experimental difficulties in obtaining sample alignment, the first attempt to measure adhesion was not made until 24 minutes after cleavage. Indications of adhesion were present, but the adhesion magnitude was below measurement capabilities ($< 10^{2}$ dynes).

Run #7 Orthoclase (001) and Labradorite (001)

The double cleavage was performed at a system pressure of 4×10^{-10} mm Hg.

During cleavage, a pressure burst to the mid 10^{-9} mm Hg range was observed. The lower sample (labradorite) cleavage surface produced was extremely irregular. The upper sample rotated so that the respective a-axes were 90° apart in rotation. Upon contact it was noted that the samples had an apparent contact area of only about one-fifth of the total cross-sectional area. The first measurement of adhesion, five minutes after cleavage, gave an adhesion force of 4×10^2 dynes. Only a small indication of a long range attractive force was observed, as a lateral ($\approx$ 0.5 mm) displacement as the samples were brought into contact. Repeated contacts caused chips to transfer between the surfaces without, however, any noticeable effect on the adhesion. The adhesion force decreased slowly until its magnitude dropped below measurable about two hours after cleavage. The data obtained are shown in Figure 17.

Study of the contact surfaces after removal from the vacuum system revealed that a considerable amount of material transfer had occurred.

Run #8 Orthoclase (001) and Albite (001)

The double cleavage was performed at a system pressure of 4×10^{-10} mm Hg. During cleavage, a gas burst to the top of the 10^{-9} mm Hg range was observed. The upper sample then rotated so that the respective a-axes were 20° apart in rotation. First contact was made two minutes after cleavage resulting in an adhesion force of 6×10^2 dynes. A small long range attractive force was observed, which had a tendency to cause a small lateral displacement as the samples were brought toward contact. The adhesion force remained about constant for several hours after cleavage. However, about five hours after cleavage it was noted that the sample alignment had changed for some reason. Previously the samples had been displaced about 1 mm laterally and rotated 90°. Now, when apart the samples were in line and rotated only 10°. As the samples were brought toward

contact it was found that the long range attractive force would restore the samples to their previous contact position. This behavior remained throughout the duration of the run. In addition, by changing the relative sample orientations, it was found that there were several positions of contact that were stable and resulted in the same adhesion force; conversely, there were several positions at which the samples would refuse to contact, displacing in all cases to one of the stable positions. The data obtained are shown in Figure 17.

The pump was then turned off and dry N_2 slowly admitted to the system. At the time of turning off the pump the adhesion force was 10^2 dynes. This force remained about constant to a system pressure of 4×10^{-6} mm Hg, beyond which its magnitude decreased below measurement capabilities. Evidence of very small adhesion persisted to about 10^{-4} mm Hg when it was no longer detectable. Re-evacuation of the system to 5×10^{-9} mm Hg did not cause the adhesion to return.

Run #9 Orthoclase (001) and Orthoclase (001)

This run represents the only double cleavage where the same mineral was used for both samples. For this run, a Varian Quadrapole Mass Spectrometer was added to the system to study the nature of the gas bursts which were found to occur for most runs.

The double cleavage was performed at a system pressure of 4×10^{-10} mm Hg. During cleavage, a gas burst to the mid 10^{-9} mm Hg was observed. Following cleavage the upper sample rotated so that the respective a-axes were 40° apart in rotation. First contact was made three minutes after cleavage giving an adhesion force of 8×10^3 dynes. A relatively strong long range attractive force was present. This force produced about a 1 mm lateral displacement of the upper sample as the samples were brought toward contact. The force decreased rapidly at first and then more slowly over the next 24 hours. At this time the force was marginally measurable and the run was terminated. The data are shown in Figure 18.

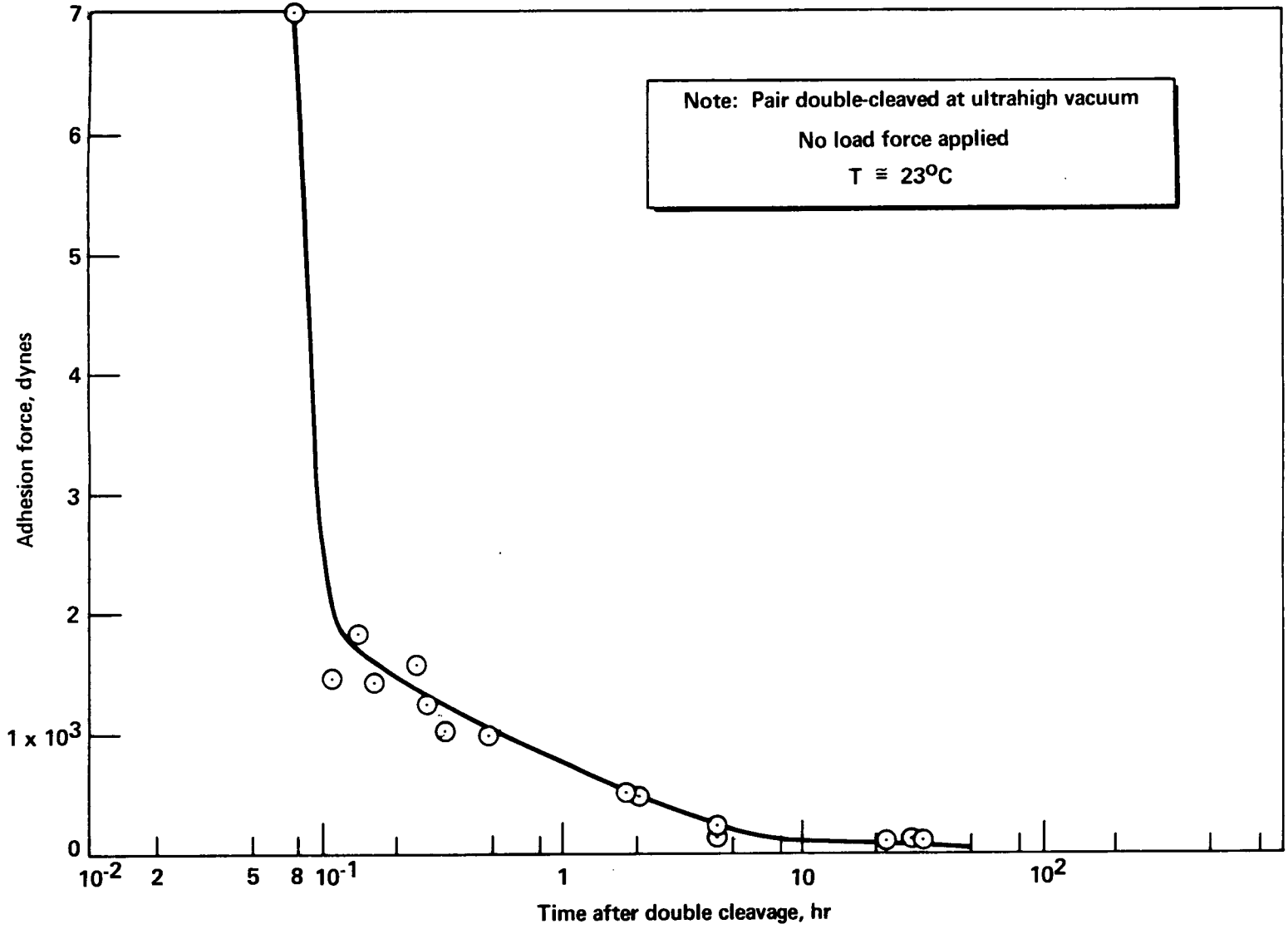

Figure 18. Adhesion Force vs Time for Orthoclase (001) Sample Pair, Run No. 9

10.0 DISCUSSION OF DATA

10.1 Air-Formed Surfaces

10.1.1 Silicate-Silicate Contact

The data for adhesion force as a function of load force for various contacting air-formed silicates are shown in Figures 3-6. Two types of adhesional behavior are evident. The first type, designated type A, is characterized principally by a very rapid rise in adhesion force as load force is increased and a lack of detectable adhesion at lower loadings. The adhesion forces are highest for this type (the scatter of data at high load appears to be due to the difficulties in keeping the samples parallel). The second type designated type B, is characterized principally by the relative insensitivity of the adhesion to the load force, measurable adhesion at very low load, and the relatively small magnitude of the adhesion force.

There are three other important differences in these two types of behavior which are not evident from the figures: the detection of adhesion in nitrogen (at atmospheric pressure), the presence of surface damage and material transfer, and the effect of surface roughness. Type A behavior was observed to persist only in ultrahigh vacuum. It was never observed before or during evacuation. After ultrahigh vacuum had been reached, admission of dry nitrogen (to atmospheric pressure) caused a rather rapid disappearance of this behavior. Direct admission of air caused immediate disappearance. Type B behavior, on the other hand, persisted in nitrogen (after previous evacuation to ultrahigh vacuum but not before), disappearing upon admission of laboratory air to the system. In every case where type A behavior was observed, surface damage was produced; also, material transfer was noted when the surfaces were of sufficiently different character for it

to be detected. This damaged and transferred material was found to adhere rather strongly to the underlaying surface and was quite difficult to remove. Figures 19 and 20 are micrographs of two of the surfaces. Figure 19 shows an orthoclase (001) surface after contact with a hypersthene (110) surface at ultrahigh vacuum (Run #3, Table 1). The intermediate albedo material is the original orthoclase surface; the lightest material consists of orthoclase chips that have been broken from the surface; the darkest material is hypersthene which has been transferred to the surface. Figure 20 shows an orthoclase (001) optically flat surface after contact at ultrahigh vacuum with another orthoclase (001) optical flat (Run #12, Table 1). Extensive surface damage is evident (brighter areas). Contrary to these findings, no surface damage was produced when only Type B behavior occurred.

A series of curves for orthoclase contacting orthoclase, at various crystalline orientations, are shown in Figures 3, 5, 6. Intercomparison of these curves, at highest load, shows that the magnitude of Type A adhesion is influenced by the crystalline orientation. Maximum adhesion occurs when the crystals are closest to being matched in orientation. Minimum adhesion occurs in the vicinity of 90° mismatch beyond which (up to about 190°) there is some evidence for an increase in the adhesion force.

Figure 5 shows the effects of surface roughness upon the adhesion. Here, surface roughness was varied from 5 microns peak to peak to 300 Å peak to peak. It is evident that Type B behavior is greatly influenced by surface roughness, the adhesion force magnitude increasing as roughness decreases. On the other hand, there is no apparent correlation between surface roughness and Type A behavior (note that though the crystalline orientations in the three runs are somewhat different they fall in the orientation range where adhesion force appears to be least sensitive to orientation change.

It appears that the forces involved in type A behavior are probably the normal

Note:
Surface after contract at ultrahigh vacuum
Dark areas are hypersthene
Light areas are orthoclase

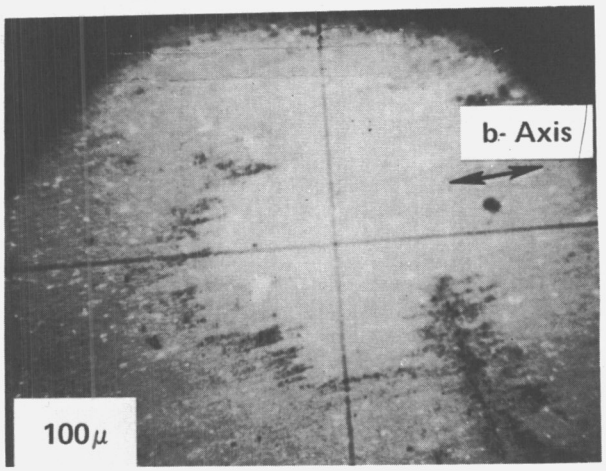

Figure 19. Transfer of Hypersthene (110) to Orthoclase (001) Air-Formed Surface, Run No. 3, Table 1

Note:
One of Two Optically Flat, Air-Formed Surfaces After Contact at Ultrahigh Vacuum
Light Regions are Areas of Surface Disruption and Material Deposition

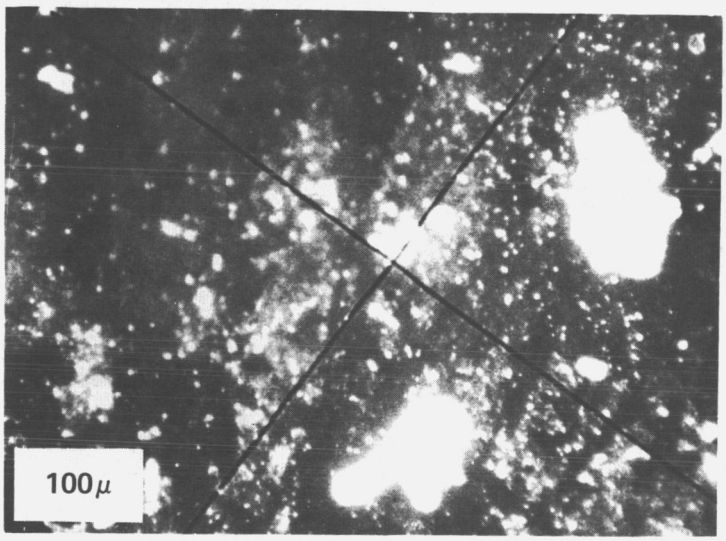

Figure 20. Micrograph of Orthoclase Surface, Run No. 12, Table 1

atomic bonding forces of the silicate lattice. The principal reasons for this conclusion are, first, the noted surface disruption and material transfer produced and, second, the fact that this behavior occurred only in ultrahigh vacuum. An additional reason is the apparent crystalline orientation sensitivity of this behavior. The normal silicate atomic bonding forces are the only forces, except possibly for mechanical effects produced by abrasion, loading-unloading, and surface roughness, that are sufficiently strong to cause surface disruption and material transfer. To exclude these alternative possibilities, the surfaces were contacted in air a number of times, then loaded, and in some cases rotated while loaded. No surface damage remotely approaching that obtained in vacuum was detected, and we thus had strong evidence that neither abrasion nor loading-unloading cycles caused the surface damage. To eliminate the possibility of surface roughness being a factor, Run #12 was made with two optically flat surfaces. These surfaces had peak-to-peak roughness of about 300 Å. It was found as noted previously (Figure 20), that even with such surfaces, extensive damage was produced. In fact, the damage was considerably greater than in any previous run, though this may be an observational effect because damage should be more easily seen against the smooth, almost flawless background surface.

The range of effectiveness of the normal silicate bonding forces is the shortest of all the forces which may act. Hence they are the most sensitive to the amount of surface contamination present. Contamination on the sample surfaces formed in air undoubtedly remained, even in ultrahigh vacuum, and it would appear from the very rapid rise in adhesion with increasing load and its disappearance at low loads that only under load was the contamination penetrated (note that the very rapid rise in adhesion with load force increase is not explainable from simple elastic-plastic deformation theory). In addition, the charge and coordination demands of the surfaces were undoubtedly initially satisfied, since they were formed in air, so that only under high load could sufficient distortion occur to make bonding sites

available. These considerations, coupled with the disappearance of type A behavior in nitrogen, air, and moderate vacuum, provide strong evidence that type A behavior is indeed caused by the normal silicate bonding forces.

The evidence indicates that type B behavior is due to dispersion forces. The principal arguments for this are (1) the inability to detect any long-range forces in vacuum, except on rare occasions, (2) the very small scatter in the experimental data, (3) the relatively small load dependence of the adhesion, (4) the ease with which the magnitude of the adhesion can be explained theoretically on the basis of dispersion forces, and (5) the notable increase in this type of adhesion as surface roughness decreases.

Homogeneous surface charging could conceivably contribute to the relatively low-magnitude adhesion forces detected for type B behavior, but it does not appear to be likely because no long-range forces could be detected. This lack of detection placed an upper bound on their effectiveness, which is much less than the observed adhesion. The very small scatter in the vacuum data indicates that neither mosaic nor homogeneous surface charging could be significant, since both of these should produce highly erratic adhesion behavior for surfaces formed in air. The relatively small load dependence of the adhesion would be expected if the dispersion forces were acting. Because of the long-range action of dispersion forces, their magnitude should not be greatly affected by microdisplacements of the surfaces toward each other under load.

As surface roughness decreases, the magnitude of the dispersion force contribution to adhesion should increase, since the surfaces come effectively into more intimate contact.

That this is the case for Type B behavior is shown in Figure 5.

Type B behavior has been found to persist in a dry nitrogen environment even at atmospheric pressure. This is consistent with the observations of previous investigators who performed their investigations at moderate vacuum and in air (with careful prior surface cleaning). The dispersion forces, being of rather long-range action, are relatively insensitive to the degree of surface contamination.

The data for adhesion force as a function of temperature are shown in Figure 7. It can be noted immediately that within the scatter of the data the adhesion force is independent of temperature over a rather wide temperature range. The two runs shown are of particular interest because Run #2 is for the orthoclase (001)/orthoclase (001) samples in the load range where type A behavior occurs and Run #5 is for the hornblende (101)/bytownite (001) samples in the load range where type B behavior occurs. The finding of the lack of a temperature dependence for type B behavior is not surprising, and indeed it would not be expected if type B behavior is, as believed, produced through the action of dispersion forces. The lack of a temperature effect for type A behavior indicates that either the physical properties of silicates do not change appreciably over this temperature range or that at the points of true contact high transient temperatures are generated, the magnitude of which is not much affected by the background temperature. Contact temperature rise undoubtedly occurs, but the degree to which this can account for the observations is uncertain. Little can be said about the former possibility because of the lack of experimental data on silicates at low temperature.

10.1.2 Silicate - Non-Silicate Contact

The data for adhesion force as a function of load force for various contacting air-formed silicates and non-silicates are shown in Figures 8-10. It is seen that the silicate-metal data are similar to the silicate-silicate data in that types A and B behavior are present. The silicate contacting non-metals (Figure 10) data, however, show a behavior intermediate between Types A and B. The phenomena observed and the conclusions reached concerning the nature of the responsible forces for silicate-silicate adhesion apply generally for the silicate-metal adhesion. They apply also for the glass and alumina adhesion though the distinction between the types of behavior is not clear (note that surface damage and material transfer occurred for both the glass and alumina runs indicating the action of the chemical bonding forces).

Figure 21 shows a magnesium surface after contact with orthoclase (001) at ultrahigh vacuum (Run #2, Table 2). A number of pits and hillocks are evident. The pits represent areas where magnesium has been plucked from the surface (and deposited on the orthoclase). The hillocks appear to represent distorted areas where the forces involved were not sufficiently strong to produce a pit. Electron microprobe analysis (courtesy Dr. L. Walters, NASA Goddard) revealed that orthoclase had been deposited in the vicinity of the pits and on the tops of the hillocks. The adhesion of the orthoclase to the magnesium was quite strong, the orthoclase resisting removal by mechanical action.

An oxide layer was present on the surface of the metals for all runs. Hence, except under higher load, the contact was between silicate and metal oxide. Penetration of the oxide layer under load could contribute to Type A behavior

Note:

After Contact With Orthoclase (001) Air-Formed Surface at Ultrahigh Vacuum
Note Pits Where Magnesium Has Been Removed From Surface, and Hillocks Where Orthoclase Has Been Deposited

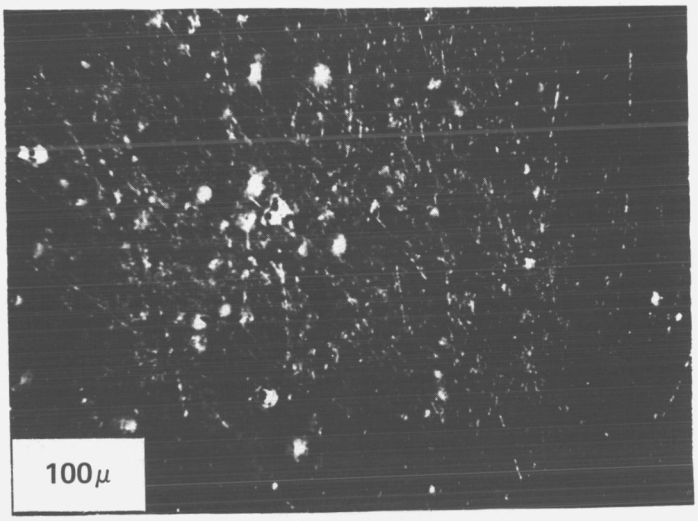

Figure 21. Pure Magnesium Surface, Run No. 2, Table 2

since then the non-directional metallic bonding forces could act. This would be particularly so for the softer metals such as the pure aluminum and magnesium, and evidence for this is seen in Figure 21.

Finally, it was found, not unexpectedly that the magnitude of the adhesion increased as the metal hardness decreased [note the series beryllium (RC50) to titanium alloy (RC29) to magnesium (RB19) to aluminum (too soft to measure)].

10.2 Vacuum-Cleaved Surfaces

10.2.1 Single Cleavage

The data for adhesion force as a function of time after cleavage, crystalline orientation, and system pressure, for single silicate cleavage, are shown in Figures 11-16. The data were obtained at room temperature and no load force was applied. A gas burst was noted for most runs during the period about cleavage. The causes of the gas bursts are discussed in Section 10.2.4. The bursts are not from the samples.

It is seen that the adhesion shows a rather rapid initial decrease after cleavage followed generally by a long period during which little change occurs. The adhesion magnitude is orders of magnitude larger than that observed for the air-formed surface runs (at low load), and in cases over an order of magnitude greater than the air-formed surface adhesion under the highest applied load.

A rather strong long range attractive force was found to be present generally (such never appeared for the air-formed samples). In many instances it was sufficiently strong to pull the samples into contact for separations less

than 1-2 mm. It was also capable of rotating and displacing the samples into their pre-cleavage match even with considerable initial mismatch after cleavage. The greatest such effect noted to date was one run where the force overcame a 30° mismatch in rotation (upper sample with respect to the lower sample) and a 1 mm lateral displacement. Additionally, it has been found that for some runs this force caused attraction to any metal in the vicinity, whereas in other runs there was no attraction. The charge also appeared to have little or no surface mobility since contact of the samples with each other or nearby metal parts did not cause any decrease in the magnitude of the adhesion.

There are three possible adhesion-producing mechanisms for the vacuum-formed surfaces. These are the action of (1) the silicate atomic bonding forces, (2) the dispersion forces, and (3) electrostatic charging (this is in contrast to the air-formed surfaces where, besides these forces, surface contamination can play a role). Of the three it can be stated with certainty that the dispersion forces make little or no contribution to the observed adhesion. This is concluded because large magnitude adhesion has appeared for runs where the surfaces produced were, inadvertantly, of extreme roughness.

Of the remaining two possibilities, it is certain that electrostatic charging is produced during surface formation. This follows indirectly, but unavoidably, from the observations of a strong long range force which could pull the samples into contact for separation up to 1-2 mm. The case for the action of the silicate atomic bonding forces, for essentially touch contact between the samples, is not so clear.

Figure 11 shows one of the runs of particular interest. Shortly after cleavage a large adhesion force was present (8×10^3 dynes). This force decreased rapidly during the next few minutes, bottoming out at a constant force which persisted essentially unchanged for an extended period. If one extrapolates backwards in time to shortly after cleavage it is seen that the adhesion force apparently was then very much larger. During the period of rapid decrease we measured, by cathetometer, the distance of sample separation at which they were pulled together, finding that this remained constant. This apparent constancy of long range force contrasted to the large decrease in adhesion indicates that during this period more than one process was acting. This initial large adhesion may be due to the action of the silicate atomic bonding forces. Additional indications that this may be the case were noted for several runs where the samples contacted surrounding system components resulting in transfer and adherence of metal to the sample. For the period following the rapid decrease, however, it appears rather definite that the surface charging is primarily, if not entirely, responsible for the adhesion.

The possible origin of this surface charging is worth note. During the initial vacuum cleavage runs we observed only a direct attraction (no rotation or displacement) which indicated that the charge was probably produced through the breakage of the atomic bonds. That is, silicates possess a number of different types of atoms (ions) and when cleavage (or fracture) occurs it is hence possible that either a random or non-random separation of ions occurs. For the samples studied the separation should be random, and hence we made some order of magnitude calculations to determine whether the observed force could be explained on this basis. It was found that a charge excess of only $\simeq 10^7$ elementary charges was required. Since $\simeq 10^{13}$ bonds were broken in the

cleavage, such a net charge is easily explanable on a random charge separation basis. However, later observations (sample rotation and displacement) indicate that the field was macroscopically anisotropic. This anisotropy cannot be explained on the basis of random charge separation due to bond breakage. Rather, it appears that the defect structures of the crystals may be the major contributors. Possible charging mechanisms related to defect mechanisms are discussed in Section 10.2.3.

Figures 13, 15 and 16 show some of the effects of crystalline orientation on the magnitude of the adhesion force. It is seen that the adhesion force is largest when the crystal axes are closest to being matched in rotation. Unfortunately this orientation effect does not serve to discriminate between the forces that could act because, as has been seen, the surface charging is macroscopically anisotropic; also, since the two faces were formed by a single cleavage they would mate better in their pre-cleavage orientation.

Figure 14 shows the effect of system gas pressure upon the adhesion force. It is seen that some small amount of adhesion can persist up to system pressures as high as 10^{-4} mm Hg; also, that the adhesion does not recover when the system is re-evacuated to the ultrahigh vacuum range. This indicates that the surface charging (primarly if not entirely responsible for the adhesion shown) is sensitive, but not critically so, upon the presence of some surface contamination. This conclusion applies only to nitrogen contamination, the gas used, and may very well not apply to gases such as oxygen and water vapor.

10.2.2 Double Cleavage

The data obtained from the double-cleavage studies are shown in Figures 17 and 18. All runs in Figure 17 are for vacuum cleaved surfaces of dissimilar silicate minerals in contact. Figure 18 shows the single run where both surfaces to be contacted were formed by ultrahigh vacuum cleavages of two samples of the same mineral. It is seen that the highest value of adhesion force occurred for the same samples in contact; also that its magnitude is the same as the maximum value obtained from single cleavage.

Comparison of Figures 17 and 18 with Figures 11-16 for single cleavage shows that the magnitudes of the adhesion and general behavior with time are similar. In addition, it was found that for both single and double cleavage a long range attractive force was present. This long range force was similar, in both cases, with respect to range of magnitude, macroscopic anisotropy, and effect of system pressure. Of particular interest was that the net force was always attractive. It had been thought that for the double cleavages there would be occassions where the net force was repulsive. Work function differences, for the dissimilar samples could conceivably cause a net electrostatic attractive force (see Section 10.2.3 for discussion). However, that apparently this is not the cause is shown in Run #9, Table 4, where the long range force between essentially identical orthoclase samples was found to be attractive. The observations indicate that the macroscopic anisotropy is the cause. That is, it was found that when the samples were brought together there were preferred positions for contact, with the samples, if possible, displacing to these positions.

It is concluded that for any comminution process occurring to silicates in ultrahigh vacuum, the products will tend to agglomerate.

10.2.3 Origin and Nature of Long Range Force

The data obtained indicate that the behavior of the long range force is rather complex and quite variable. Considering all runs to date we find that for some the samples are attracted to any metal in the vicinity; for others no attraction is evident. For some runs the force field appears to be sufficiently anisotropic to rotate and displace the samples into apparent atomic match even when a significant mismatch initially exists; for other runs no such behavior occurs. For some runs this force appears to be practically non-existent, yet significant adhesion is present; for other runs it is quite strong. For one run it persisted to a system pressure of about 10^{-5} mm Hg and for another to about 10^{-4} mm Hg.

Since this force contributes significantly to the observed adhesion it is worth considering its possible origin(s), and discussing various experiments which can perhaps bring an understanding as to why it behaves as it does, and the extent to which it actually contributes to the total adhesion.

The long range nature of this force indicates rather definitely that the force is produced through surface electrostatic charging. When a crystal is cleaved (or fractured) it is to be expected that surface charging will be produced, associated with the breakage of the atomic bonds. This process can in some instances be non-random, with each face preferentially receiving a net and opposite charge, or it can be random with the tendency being for

each surface to end up with zero net charge (though a net charge can be produced in this case also, due to statistical fluctuations about the null point). Though it appears, for the silicates we have been studying, that the charge separation should be essentially random, rough calculations, reported in previous quarterly reports, indicate that the observed magnitude of the long range force can be easily explained on the bases of either random or non-random charge separation. However, this general mechanism of surface charging cannot account for the evident macroscopic anisotropy of the force field noted for many of the runs. Hence we must search for other charging mechanisms which may be contributing.

Three characteristics of real crystals which can produce surface charging phenomena are crystalline dislocations, non-uniform composition, and the crystal work function (when dealing with dissimilar materials). These are discussed in the following sections.

10.2.3.1 Crystal Imperfections

All the crystals studied to date possess a center of symmetry and hence are not piezoelectric. However, a second order piezoelectric effect could occur, associated with the crystal defect structure. Also, charges could be produced through polarization caused by the migration of charged dislocations during precleavage deformation or during the cleavage process itself.

Edge dislocations are charged in ionic crystals and are surrounded by a compensating charge cloud attached to a variety of crystalline trapping levels. When the edge dislocations move in a stress field the charge on the dislocation moves with it leaving behind the compensating charge cloud.

If the lifetime of the trapping levels is sufficiently long, a polarization $\overline{P}$ is produced which will give an electrostatic surface charge if the cleavage plane intersects the polarization field. The net charge will be proportional to $\overline{P} \cdot \overline{n}$ where $\overline{n}$ is the cleavage plane normal.

A second effect (which is a real piezoelectric effect) is due to the assymetry of the edge dislocation. Since it lacks a center of symmetry, a stress field (permanent or transient due to cleavage) will produce a polarization if there is an excess of positive or negative dislocations. A deformed sample which has undergone bending and subsequent polygonization will satisfy this condition. Again, the intersection of the cleavage plane and the polarization field will leave a net, equal and opposite, charge on the new faces produced.

There is a final effect which is partly related to the previous two. Over and above the net charging produced at the kinks of an edge dislocation composed of more than one atomic species, the larger of the two ions will tend to move into the dilation region of the stress field with the smaller staying in the compressional region. The final configuration is a line dipole colinear with the edge dislocation together with a compensating dipolar charge cloud. An excess of positive or negative dislocations produces a net polarization field which in turn provides a net surface charge when the cleavage plane does not coincide with the neutral plane of the dipole array.

10.2.3.2 Non-Uniform Composition

Any crystal which has a non-uniform composition (due either to stoichiometry

or impurity gradients) has a built in electric field associated with the transition zone. The electric field compensates the diffusion force due to the charge carrier concentration gradient. Therefore a cleavage plane through an inhomogeneous crystalline region passes through a corresponding polarization field.

10.2.3.3 Work Function

A surface charging can be produced between dissimilar materials whose work functions are different since there will be a transfer of electrons which equalizes the fermi levels in the materials in contact. The force will always be either zero or attractive. However if the work function attractive force is coupled with one or both of the previous effects, complex electrostatic attraction-orientation effects can be expected.

10.2.4 Source of Gas Bursts

It was found, during the operations involved with cleavage, that gas bursts almost invariably occurred. These were sufficient to temporarily raise the system pressure, in some instances, to the base of the 10^{-8} mm Hg range. One possible source of these bursts could be the sample itself, but the large magnitude of the bursts made it difficult to believe that the sample was responsible. Accordingly, tests were made where all mechanical operations associated with the cleavage, except the cleavage itself, were performed. It was found that identical gas bursts were obtained. Tapping the vacuum chamber in various areas also produced similar bursts. In particular, it was found that the ion pump diodes were most sensitive to the tapping. It was therefore concluded that 1) the bursts were not from the sample, and 2) the bursts were either due to gas released from the chamber walls during vibration, or more probably from the pump diodes.

A Varian Quadrapole Residual Gas Analyzer, loaned to us by Varian, was attached to the system adjacent to the sample to be cleaved. Spectra were taken of 1) the residual gases in the pumped system at 3×10^{-10} mm Hg, 2) the gases found in the gas bursts resulting from tapping the system and pump diodes, and 3) the gases found in the gas burst occurring during cleavage.

It was found that the principal background gases at 3×10^{-10} mm Hg consisted of H_2, He, CO, A, N_2 and CO_2, with slight traces of F and Cl. No peaks above a mass to charge ratio of 44 were seen. Tapping the chamber walls and pump diodes resulted in an appreciable increase in the amounts of H_2, He, CO, and A present. CH_4 also appeared and some additional CO_2 may have been released. The presence of increased amounts of H_2 and CO are highly indicative that the gases released come from the stainless steel chamber walls and pump body. The spectrum during cleavage appears to be identical to that produced by tapping the system, providing further evidence that the observed gases are not coming from the sample.

Nevertheless, the bursts did cause contamination of the sample surfaces. The He and A, being inert, are of no great concern. However, the H_2, CH_4, and CO can affect the adhesion, reducing its magnitude over that which would be present if the surfaces were ultraclean.

11.0 IMPLICATIONS OF RESULTS TO THE MOON

It has been noted previously that the surfaces of lunar material could range from ultra-clean to contaminated. The findings of this study demonstrate that the adhesional behavior of silicates, believed to comprise the bulk of the lunar surface material, is critically dependent upon the surface state. Hence, it can be expected that the adhesion problems encountered on the Moon can vary widely, due to lateral or temporal changes in the surface state produced either through the action of the Moon's natural environment or through the operations of man.

11.1 Lunar Soil Mechanics

The Surveyors have shown that the lunar materials do adhere and that, at least in the vicinity of the landing sites, there are no bearing capacity problems. These findings are in accord with those of the present study. The present study, additionally, provides information as to the possible variation in soil properties that could be produced by adhesion.

The magnitude of the adhesion between the soil grains required to account for the Surveyor observations is very roughly that obtained for the contaminated samples after the application of moderate load; also roughly that found to persist after vacuum cleavage (the surfaces contaminated to some degree). The implications are therefore that some contamination is present on the lunar grain surfaces. This contamination may have been present prior to the Surveyor landing, but contamination was certainly introduced by Surveyor. Because of the Surveyor contamination it is apparent that insofar as the Surveyor sites are "typical" the general adhesion of the surface material is at least as great as that observed by Surveyor and indeed may be significantly greater.

It is possible that there are areas on the surface where the adhesion is much less than in the Surveyor landing areas. The adhesion could be less where the soil has not been loaded to any significant degree, or a very large amount of adhesion-reducing contamination is present. Such areas would probably constitute only a very small fraction of the surface because 1) the primary soil production agency is likely to be (micro) meteorite impact so that unless a horizontal soil transport mechanism (other than impact) were active it is difficult to envisage any significant fraction of the soil that has not been loaded, and 2) Surveyor has shown that the general surface contamination, including that from Surveyor, is not sufficient to eliminate adhesion so that only in limited areas where appreciable gas of internal origin may be released could adhesion be reduced over that found.

Adhesion contributes to soil strength. The pertinent relation is

$$s \cong p \tan \phi + c$$

where s is the soil shear strength, a measure of how well the soil will support external load, p is the load normal to the potential failure plane, c is the cohesion (adhesion), and ϕ is the angle of internal friction. The quantity ϕ is primarily a function of grain shape, porosity, and mechanical friction; increasing as grain angularity increases, as porosity decreases, and as mechanical friction increases. The quantity c, in the terrestrial sense, is the attractive interaction between soil grains due to the presence in the soil of water, with its various dissolved electrolytes. The terms "ϕ" and "c" are two of the important parameters in soil mechanics. In general, as ϕ and c increase, the problems related to soil behavior under load decrease.

The quantities c and ϕ for terrestrial soils are found to be essentially independent of load, and in the above equation they are treated as constants. However, the present study has shown that the adhesion (cohesion) of lunar soils should be highly load dependent and hence that c, for lunar soils, will not be constant. The results also imply that ϕ may not be a constant. These findings indicate that great care must be taken in applying terrestrial soil mechanics equations to predict the engineering behavior of lunar soils.

It has been found that a considerable amount of surface charging is produced when a fresh silicate surface is formed in ultrahigh vacuum. The net resultant force was always attractive. Hence, during any comminution process on the Moon (not involving the release of contaminent gases) the surface charging produced should cause agglomeration of the newly formed soil. This cohesion should be large, in fact possibly larger on the Moon than observed in the experiments due to the expected greater defect density of lunar material. This charging, however, cannot contribute significantly to the cohesion over an extended period of time. The reasons are 1) the charge will decay slowly, over a period of several days to weeks due to the non-zero electrical conductivity of silicates, and 2) the galactic and solar cosmic rays, the solar wind, and the solar photons (UV, X-rays) will act as discharging mechanisms.

11.2 General Problems to Engineering Operations

The results of this study have shown that adhesion is critically dependent upon surface state. Hence, one is ill advised to make any general statements regarding the magnitude of lunar adhesion and the degree to which it poses a problem to lunar operations. Rather, one must first specify what operation is

to be performed. For instance, if we wish to determine the adhesion problems posed to a man walking across the surface we must ask: are the surface materials initially clean or contaminated; what is the material of his boot in contact with the surface; how much abrasion of the boot and surface material can be expected; what are the amounts, types and source locations of the gases released from his suit; and finally, will he just walk over the surface or will other operations be performed (such as breaking off rock samples, thereby producing fresh surfaces)? Probably the most important of these questions concerns the emissions of gas from his suit since this may well be the primary mechanism determining the adhesional behavior encountered (oxygen and water vapor are of particular importance since the surface is likely to be oxygen deficient). If, on the other hand we wish to drill into the surface we must ask ourselves the technique to be used, the drill materials, and the temperatures that may be generated. Drilling falls into the general class of operations which must involve production of fresh surfaces and hence for which adhesion should pose the greatest problem.

Since adhesion phenomena depend so greatly on the particular conditions and the operations to be performed, discussion of what might occur in given instances can become rather involved. Nevertheless, some general statements can be made:

(1) The adhesion of lunar material will not in general be a major problem on the Moon provided the following two conditions are met: a) all material surfaces in contact are contaminated, and b) the operations performed do not remove the contamination nor load the lunar material to any large degree.

If these conditions are met the adhesion will be caused primarily if not entirely by the dispersion forces and the magnitude of

the adhesion, considering the grain irregularity and the surface roughness of the majority of engineering surfaces, will be small. The only possible difficulties would involve optically flat surfaces and those used to produce vacuum (or air) tight seals. If these conditions are violated then the importance of adhesion can be expected to increase greatly. The case where clean surfaces are produced is discussed below. If the surfaces are heavily loaded the adherance of the soil to engineering materials will increase greatly and material transfer and surface disruption will occur. This surface disruption and material transfer is of particular importance to critical components such as optical and thermal control surfaces which indicates that during removal of soil material deposited on these surfaces great care should be taken not to apply load force (i.e. mechanical removal techniques should be avoided if possible).

(2) Lunar material adhesion can become a major problem if: a) the soil surfaces are ultraclean, b) the engineering material surfaces are cleaned by mechanical abrasion or sputtering, or c) the operations performed produce fresh surfaces.

The magnitude of the adhesion in this case will be much larger than for the contaminated surface case and the general problems correspondingly more severe. In addition, a considerable amount of surface electrostatic charging can be expected. This long range electrostatic force, in particular, will make it difficult to remove adhering material by mechanical means.

12.0 CONCLUSIONS

This report has summarized the results obtained during the past three years on a study of the ultrahigh vacuum adhesion of silicates as related to the lunar surface. Two types of silicate surface preparation were used. The first type consisted of forming the surface in air; the second type consisted of forming the surface at ultrahigh vacuum by cleavage. These two types of surface preparation were chosen to represent possible bounds to the types of silicate surface which may be found on the moon, the first type representing the contaminated surface case and the second type representing the clean surface. Adhesion force was measured as a function of load force, temperature, surface roughness, type of material, crystalline orientation, and degree of surface cleanliness.

The following general conclusions apply:

a. Two types of adhesion are present for the air-formed surfaces. The first type appears at low load, is of relatively low magnitude, and is most probably produced by the action of the dispersion forces. The second type appears under higher load, is of much greater magnitude, and is most probably produced by the action of the normal silicate atomic bonding forces.

b. The adhesion between ultrahigh vacuum-formed surfaces is very much larger than that between air-formed surfaces. The highest magnitude adhesion appears to be due to the action of the normal silicate atomic bonding forces.

c. A relatively strong long range attractive force is almost always present when the surfaces are formed in ultrahigh vacuum. This force is indicative of considerable surface charging. Its apparent macroscopic anisotropy implies that its source may well be associated with defects (dislocations and impurities) in the crystalline structure.

d. The adhesional behavior of silicates has been found to be critically dependent upon their surface state. Hence, it can be expected that the adhesional behavior found by lunar missions will be highly dependent upon how these missions (and operations) affect the surface.

e. If the lunar material surfaces are clean or have been loaded, adhesion can contribute significantly to soil strength and in general there should be no bearing capacity problems. Alternatively, if the surfaces are contaminated and have not been loaded appreciably, adhesion will contribute little to soil strength.

f. The principle problems posed to lunar missions by silicate adhesion should be those associated with contamination of critical components such as vacuum-tight doors, working mechanical parts, and optical and thermal control surfaces.

This study represents the first attempt to obtain a quantitative understanding of the mechanics of silicate adhesion. Though much has been learned, much remains to be done before we can conclude that a full understanding has been obtained.

REFERENCES

Bell, P. B., Vacuum welding of olivine, Science, 153, 410-411, 1966.

Blum, P., J. R. Roehrig, and M. J. Hordon, Properties of powder ground in ultrahigh vacuum, NASA CR-66276, National Research Corp., March 1967.

Bradley, R. S., The cohesive force between solid surfaces and the surface energy of solids, Phil. Mag., 13, 853-862, 1932.

Bryant, P. J., L. H. Taylor, and P. L. Gutshall, Cleavage studies of lamellar solids in various gas environments, Trans. 10th Natl. Vacuum Symp., pp. 21-26, The Macmillan Company, New York, 1963.

Derjaguin, B. V., A. S. Titijevskaya, I. I. Abrocossova, and A. D. Malkina, Investigations of the forces of interaction of surfaces in different media and their application to the problem of colloid stability, Discussions Faraday Soc., 18, 24-41, 1954.

DeVore, G. W., Compositions of silicate surfaces and surface phenomena, Contrib. Geol., 2, 21-37, 1963.

Eitel, W., Silicate Science: Volume I, Silicate Structures; Volume II, Glasses, Enamels, Slags, Academic Press, New York, 1964.

Grim, R. E., Clay Minerology, McGraw-Hill Book Company, New York, 1953.

Grossman, J. J., Distribution of surface electrostatic charging on dielectrics cleaved in vacuum: theoretical, presented at Adhesion of Materials in Aerospace Environments Symposium, Toronto, Canada, May 1967.

Gruver, R. M., Atomistic approach to the adhesion to glass, Glass Ind., 37, 77-80, 94, 100, 101, 1956.

Halajian, J. D., The case for a cohesive lunar surface model, Rept. ADR04-04-642, Grumman Aircraft Engineering Corp., Bethpage, N. Y., June 1964.

Harper, W. R., Adhesion and charging of quartz surfaces, Proc. Roy. Soc. London, 231, 388-403, 1955.

Johnson, R. W., and J. M. Greiner, Chemical bonding and shear strength of silicate systems under lunar conditions, paper presented to the Fourth Annual Meeting, Working Group on Extraterrestrial Resources, Colorado Springs, Colorado, November 30-December 2, 1965.

Jordan, D. W., The adhesion of dust particles, Brit. J. Appl. Phys., 5, S194-198, 1954.

Lowe, H. J., and D. H. Lucas, The physics of electrostatic precipitation, Brit. J. Appl. Phys., 4, S40-47, 1953.

Overbeek. J. Th. G., and M. J. Sparnaay, London-Van der Waals attraction between macroscopic objects, Discussions Faraday Soc., 18, 12-24, 1954.

Ryan, J. A. and F. W. Sun, Quantitative measurements of ultrahigh vacuum silicate adhesion, Trans. Amer. Geophys. Union, 46, 428, 1965a.

Ryan, J. A. and F. W. Sun, Silicate ultrahigh vacuum adhesion, Trans. Amer. Geophys. Union, 46, 546, 1965b.

Ryan, J. A., Ultrahigh vacuum silicate adhesion, J. Geophys. Res., 71, 4413-4425, 1966.

Ryan, J. A., Cohesive properties of lunar soils as indicated by Surveyor I, in Interpretation of Lunar Probe Data, 14, Science and Technology Series, AAS, 1967.

Ryan, J. A. and M. B. Baker, The adhesion of air and vacuum formed silicate surfaces, presented at Adhesion of Materials in Aerospace Environments Symposium, Toronto, Canada, May 1967, to be published by ASTM, 1967.

Ryan, J. A. and W. M. Hansen, Adhesion of ultrahigh vacuum cleaved silicates; and the Moon, presented at 48th Annual Meeting of the Amer. Geophys. Union, April 17-20, 1967.

Salisbury, J. W., P. E. Glaser, B. A. Stein, and B. Vonnegut, Adhesive behavior of silicate powders in ultrahigh vacuum, J. Geophys. Res., 69, 235-242, 1964.

Smith, H. I. and M. S. Gussenhoven, Adhesion of polished quartz crystals under ultrahigh vacuum, J. Appl. Phys., 36, 2326-2327, 1965.

Stein, B. A. and P. C. Johnson, Investigation of soil adhesion under high vacuum, in The Lunar Surface Layer, edited by J. W. Salisbury and P. E. Glaser, pp. 93-105, Academic Press, New York, 1964.

Stone, W., Some phenomena of the contact of solids, Phil. Mag., 9, 610-620, 1930.

Tomlinson, G. A., Molecular cohesion, Phil. Mag., 6, 695-712, 1928.

Tomlinson, G. A., Further experiments on the cohesion of quartz fibers, Phil. Mag., 10, 541-544, 1930.

Weyl, W. A., Wetting of solids as influenced by the polarizability of surface ions, in Structure and Properties of Solid Surfaces, edited by R. Gomer and C. S. Smith, pp. 147-184, University of Chicago Press, 1955.

NASA-Langley, 1968 — 30 CR-1090

"The aeronautical and space activities of the United States shall be conducted so as to contribute . . . to the expansion of human knowledge of phenomena in the atmosphere and space. The Administration shall provide for the widest practicable and appropriate dissemination of information concerning its activities and the results thereof."

—NATIONAL AERONAUTICS AND SPACE ACT OF 1958

NASA SCIENTIFIC AND TECHNICAL PUBLICATIONS

TECHNICAL REPORTS: Scientific and technical information considered important, complete, and a lasting contribution to existing knowledge.

TECHNICAL NOTES: Information less broad in scope but nevertheless of importance as a contribution to existing knowledge.

TECHNICAL MEMORANDUMS: Information receiving limited distribution because of preliminary data, security classification, or other reasons.

CONTRACTOR REPORTS: Scientific and technical information generated under a NASA contract or grant and considered an important contribution to existing knowledge.

TECHNICAL TRANSLATIONS: Information published in a foreign language considered to merit NASA distribution in English.

SPECIAL PUBLICATIONS: Information derived from or of value to NASA activities. Publications include conference proceedings, monographs, data compilations, handbooks, sourcebooks, and special bibliographies.

TECHNOLOGY UTILIZATION PUBLICATIONS: Information on technology used by NASA that may be of particular interest in commercial and other non-aerospace applications. Publications include Tech Briefs, Technology Utilization Reports and Notes, and Technology Surveys.

Details on the availability of these publications may be obtained from:

SCIENTIFIC AND TECHNICAL INFORMATION DIVISION

NATIONAL AERONAUTICS AND SPACE ADMINISTRATION

Washington, D.C. 20546